IMPACT OF SMALL-X EVOLUTION ON NUCLEAR DEFORMATION & APPLICATION TO ISOBAR COLLISION

PRAGYA SINGH - JYVÄSKYLÄ UNIVERSITY

BASED ON THE ONGOING WORK WITH G. GIACALONE, B. SCHENKE AND S. SCHLICHTING

INTERSECTION OF NUCLEAR STRUCTURE AND HIGH ENERGY COLLISIONS , INT

UNIVERSITY OF JYVÄSKYLÄ

ACADEMY OF FINLAND

Outline

1. Introduction
2. Methodology
   - Quantum Evolution
   - JIMWLK on lattice
3. Results
   - Effect of JIMWLK on bunch of nuclei (U, Ne, Zr, Ru)
4. Conclusion
   - Summary & Future Prospects

Characterisation of Heavy-ion collisions

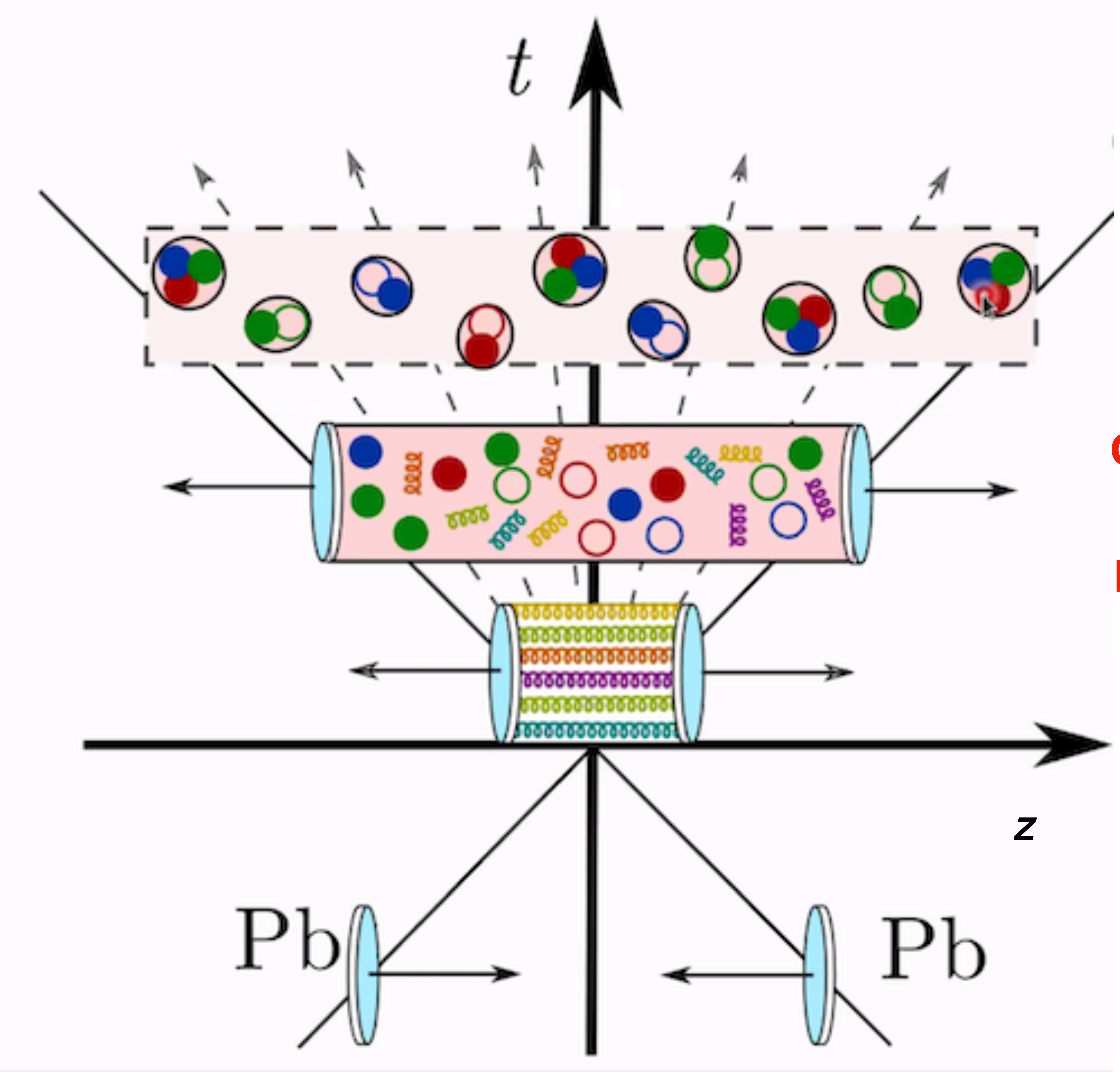

Hadronic Gas $(\tau \approx 10 - 15 \text{ fm/c})$
Kinetic Theory

Quark Gluon Plasma $(\tau \approx 1 - 10 \text{ fm/c})$
Viscous hydrodynamics

Non-eq. Evolution $(\tau \approx 0.2 - 1 \text{ fm/c})$
Kinetic theory

Energy Deposition
$(\tau \lesssim 0.2 \text{ fm/c})$
Classical dynamics

Before collision
Color Glass condensate

Our focus will be on initial energy deposition.

Artwork: Aleksas Mazeliauskas

Light-cone kinematics

- Let z be the longitudinal axis of the collision. For an arbitrary 4-vector v^μ, the light cone coordinates are

$$v^+ \equiv \frac{1}{\sqrt{2}}(v^0 + v^3) \qquad v^- \equiv \frac{1}{\sqrt{2}}(v^0 - v^3) \qquad \mathrm{v} \equiv (v^1, v^2)$$

- Invariant scalar product of two 4-vectors

$$\begin{aligned} p\,.\,x &= p^0x^0 - p^1x^1 - p^2x^2 - p^3x^3 \\ &= p^-x^+ + p^+x^- - \mathbf{p}\,.\,\mathbf{x} \end{aligned}$$

- p^- should be interpreted as LC energy and p^+ as LC momentum

Light-cone kinematics

- We define rapidity as

$$y = \frac{1}{2}\ln\left(\frac{k^+}{k^-}\right) = \frac{1}{2}\ln\left(\frac{2\mathrm{k}^{+2}}{\mathrm{m}_\perp^2}\right)$$

where for particles on the mass shell $k^\pm = (E \pm k_z)/\sqrt{2}$ with $E = (m^2 + \mathbf{k}^2)$

$$k^+k^- = \frac{1}{2}(E^2 - k_z^2) = \frac{1}{2}(k^2 + m^2) \equiv m_\perp^2$$

- For a parton inside a right-moving (in the +z direction) hadron, we introduce the longitudinal momentum fraction x

$$x \equiv \frac{k^+}{P^+}$$

The McLerran-Venugopalan (MV) model

- Consider a nucleus in the infinite momentum frame with $P^+ \to \infty$ with infinite transverse extent of uniform nuclear distribution.

- Partons with large-x or valence partons are Lorentz contracted. Nucleon appears essentially two-dimensional.

- The wee partons with longitudinal momentum fractions $x \ll 1$ are delocalized in the x^- direction

- Wee partons sees the valence partons as infinitely thin sheets of color charges

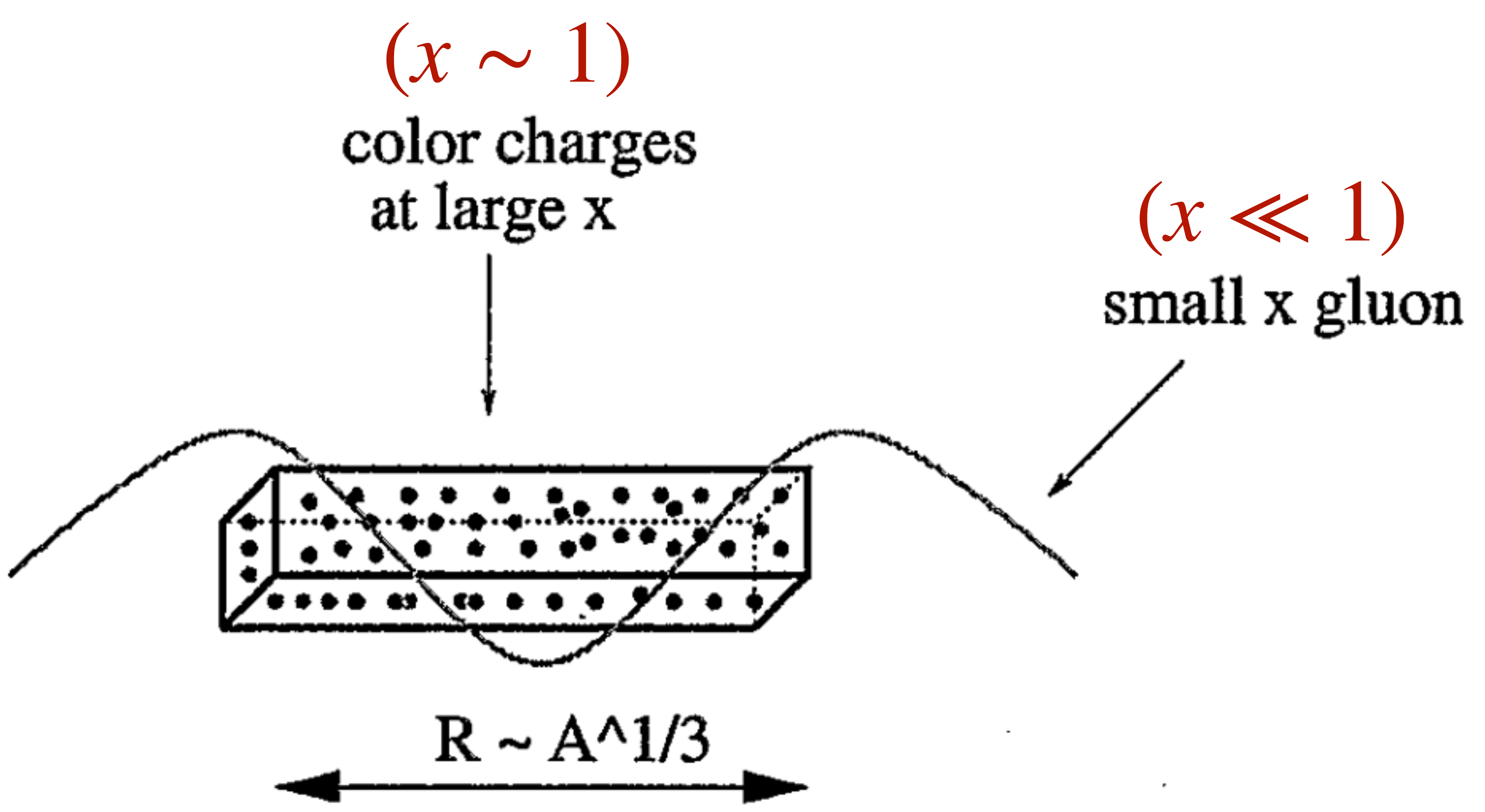

The McLerran-Venugopalan (MV) model

- Wee partons have very short lifetimes

$$\Delta x^+ \sim \frac{1}{k^-} = \frac{2k^+}{m_\perp^2} = \frac{2xP^+}{m_\perp^2}$$

➡ **Valence partons act as a source of static color charges.**

- Large-x partons are recoilless source of color charges.
- In the ultra relativistic limit, the color current is proportional to $\delta(x^-)$ and is given as

$$J^{\mu,a} = \delta^{\mu +}\delta(x^-)\rho^a(\mathbf{x})$$

where $\rho^a(\mathbf{x})$ is the color charge density

Generating color charge density

- An external probe interacts with the nucleus and resolves distance of size Δx in the transverse plane.
- The probe simultaneously couples to partons from other uncorrelated nucleons.
- Number of these sources are given as a product of density of valence quarks in the transverse plane and the transverse area.

$$N = n\Delta S_\perp = \frac{N_c A}{\pi R^2} S_\perp \sim \frac{\lambda_{\rm QCD}^2}{Q^2} N_c A^{1/3}$$

where Q^2 is the resolution and $R = R_0 A^{1/3}$ with $R_0 \sim \lambda_{\rm QCD}^{-1}$

- Based on central limit theorem, the color charge density will have a simple Gaussian probability distribution.

$$\langle \rho^a(x_\perp) \rangle = 0$$
$$\langle \rho^a(x_\perp) \rho^b(y_\perp) \rangle = g^2 \mu^2 \delta^{ab} \delta^{(2)}(x_\perp - y_\perp)$$

where μ^2 is the average color charge squared of the valence quarks per unit transverse area

Towards an effective theory

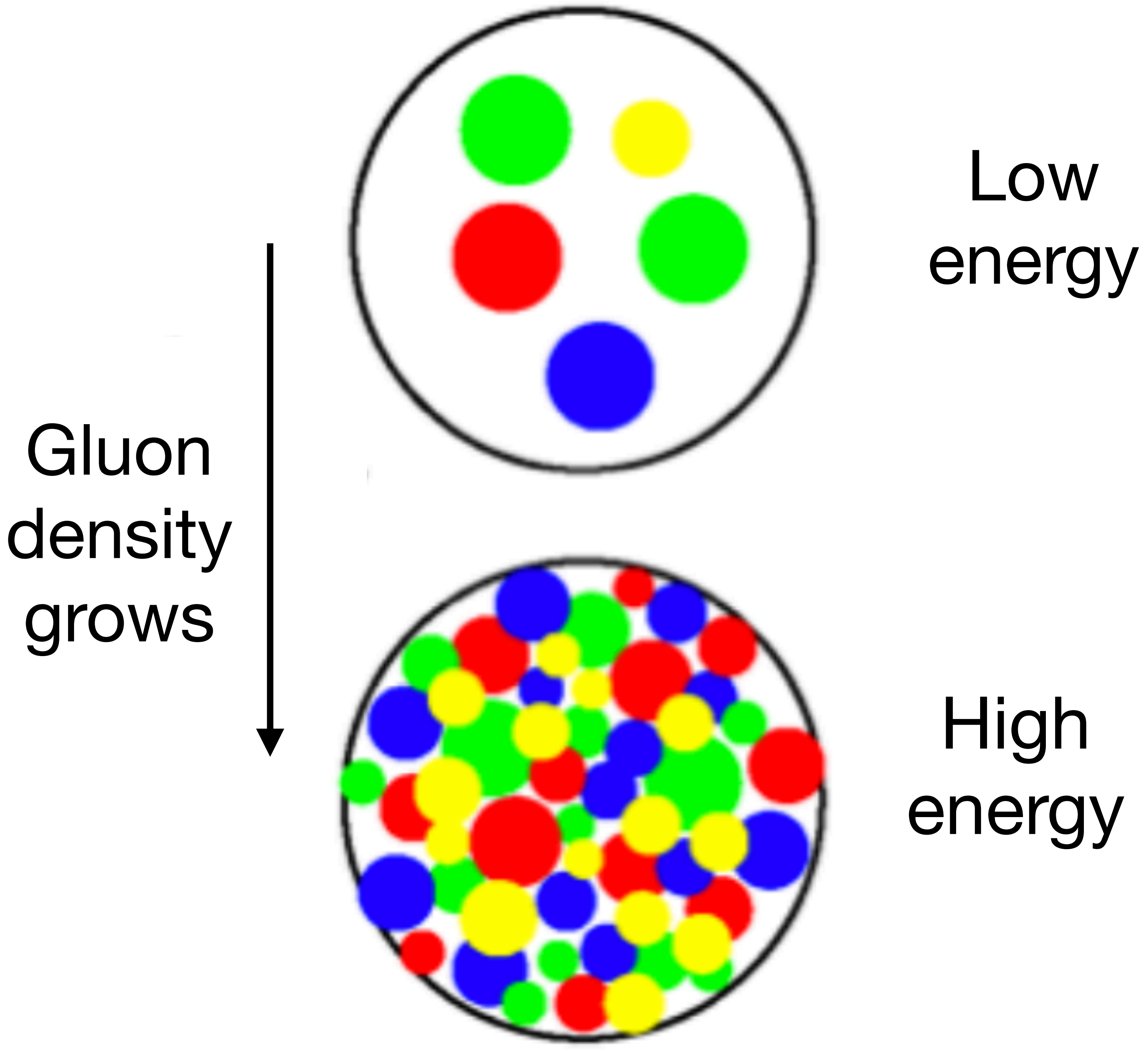

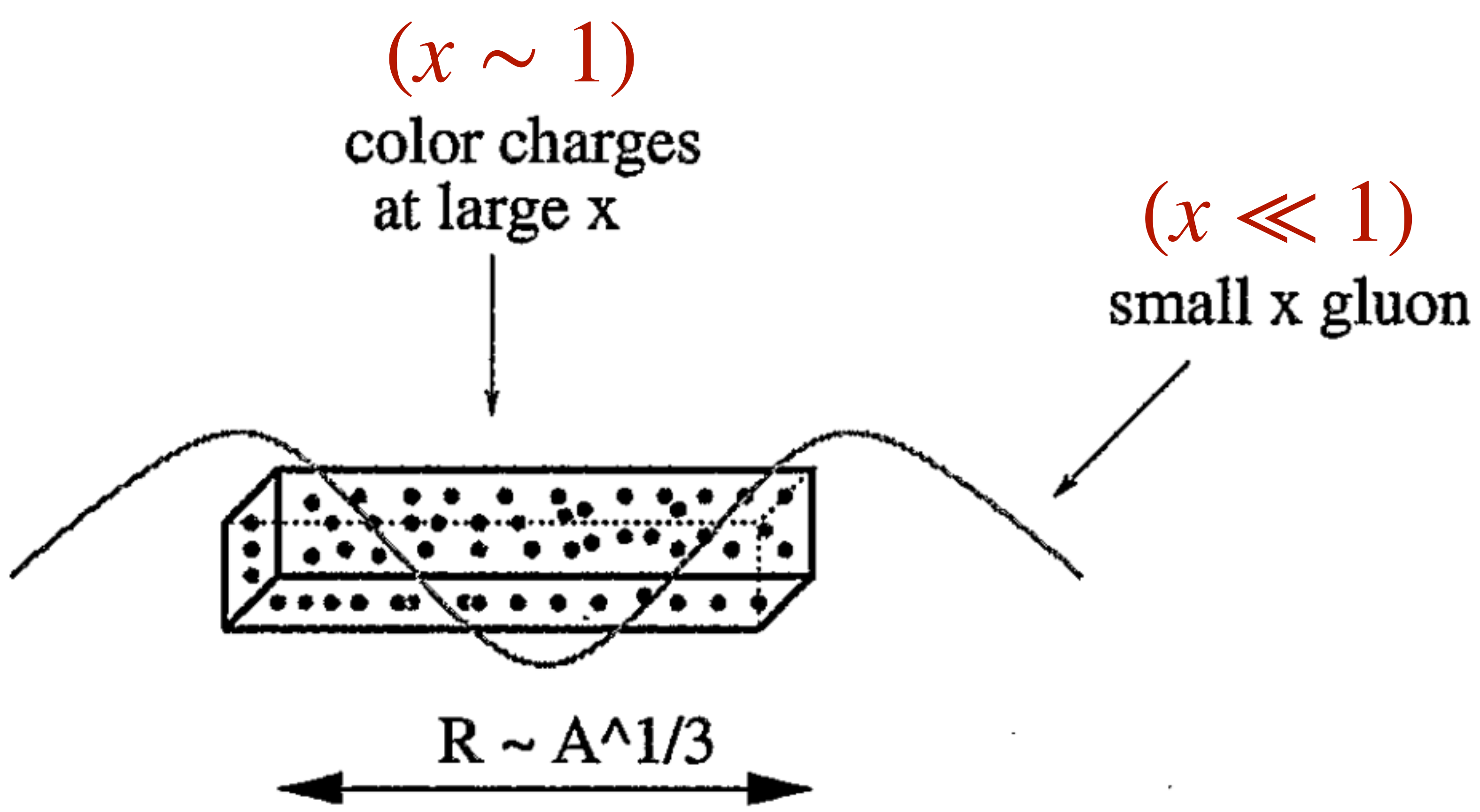

$$x = \frac{p^+}{P^+} \equiv \text{Parton momentum fraction}$$

Valence quarks— large x (x ~ 1) partons

Temporal extent $\Delta x^+ \sim \frac{2xP^+}{k_\perp^2}$

Longitudinal extent $\Delta x^- \sim \frac{1}{xP^+}$

Non-linear effect at sufficiently small-x, tames the growth

$\Rightarrow$ **Gluon saturation**

Characterised by scale Q_s (saturation scale)

$$Q_s^2 \sim (A/x)^{1/3}$$

Color Glass Condensate: Sources and Fields

iv.org/pdf/hep-ph/0406169.pdf

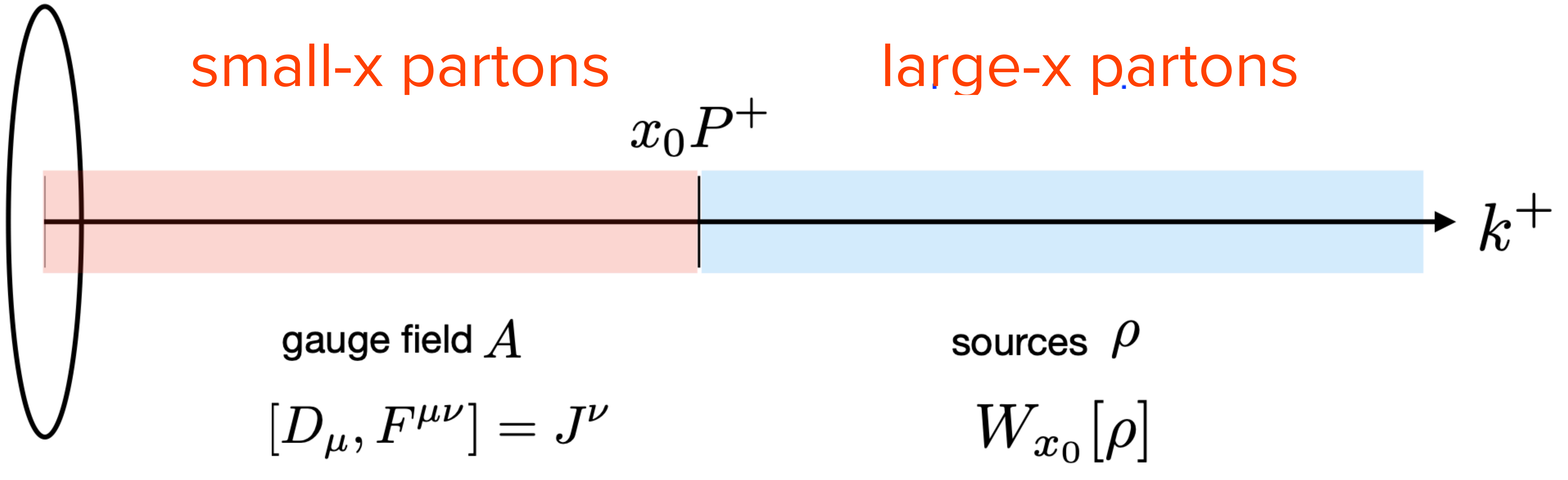

- The fast color sources are represented by the color currents $J_a^\mu = \delta^{\mu +}\rho_a$ where ρ_a are taken to be random and static
- The small-x gluons are the color fields generated according to the Yang-Mills equation

$$[D_\mu, F^{\mu\nu}] = J^\nu$$

$$D_\mu = \partial_\mu - igA_\mu^a T^a \qquad\qquad (T^a)_{bc} = -if_{abc}$$

- Observables are first computed for a fixed configuration of the color sources, and then averaged over all the possible configurations with some probability distribution $W_{x_0}[\rho]$

Wilson Lines

Interaction of high energy color-charged particle with large k^- momentum (and small $k^+ = \frac{k_T^2}{2k^-}$)

with a classical field of a nucleus can be described in the **eikonal approximation:**

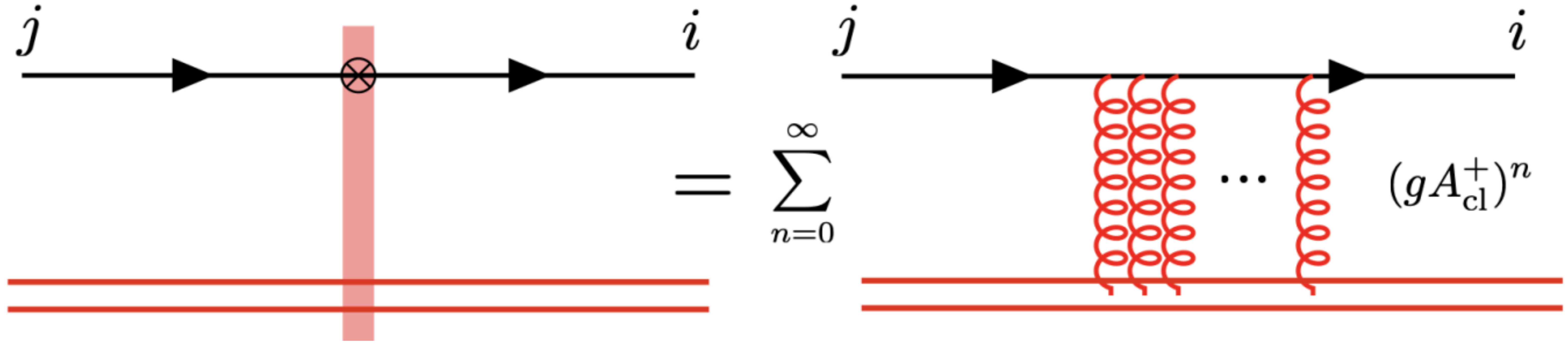

The color rotation is encoded in a light-like Wilson line, which for a quark reads

$$V(x_T) = \mathscr{P}\left(ig\int_{-\infty}^{\infty} dz^- A^{+,c}(z^-, x_T)t^c\right)$$

Path ordered exponentials

SU(3) generators in fundamental representation

Wilson lines

For a gluon interacting with the target,

$$U(x_T) = \mathscr{P}\left(ig\int_{-\infty}^{\infty} dz^- A^{+,c}(z^-, x_T)T^c\right)$$

SU(3) generators in adjoint representation

Wilson lines are the building blocks of CGC.

Wilson lines and dipole correlator

Wilson lines are building blocks of CGC. For eg, the total DIS cross section of a virtual photon scattering off a nucleus is given as

$$\sigma_{\lambda}^{\gamma^* A}(x, Q^2) = 2\int \mathrm{d}^2\boldsymbol{r}_\perp \mathrm{d}^2\boldsymbol{b}_\perp \int_0^1 \mathrm{d}z \left|\Psi_\lambda^{\gamma^*}(\boldsymbol{r}_\perp, Q^2, z)\right|^2 \left[1 - S_x^{(2)}\left(\boldsymbol{b}_\perp + \frac{\boldsymbol{r}_\perp}{2}, \boldsymbol{b}_\perp - \frac{\boldsymbol{r}_\perp}{2}\right)\right]$$

where

$$S_{x_0}^{(2)}(\boldsymbol{x}_\perp, \boldsymbol{y}_\perp) = \frac{1}{N_c}\left\langle \mathrm{Tr}\left[V(\boldsymbol{x}_\perp)V^\dagger(\boldsymbol{y}_\perp)\right]\right\rangle_{x_0}$$

$$\gamma^* \to q\bar{q} : \psi_\lambda^{\gamma^*}(r_\perp, Q^2, z)$$

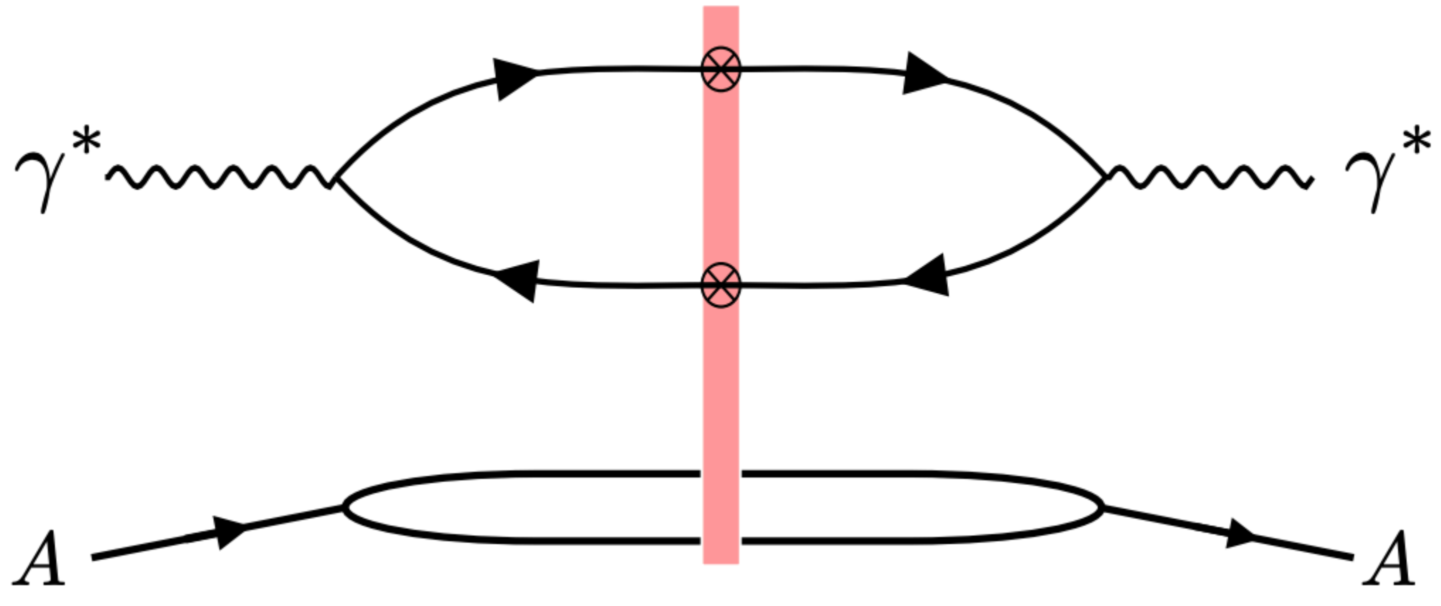

$Q^2 = -q^2$ and λ are virtuality and polarization of photon.

$$r_\perp = x_\perp - y_\perp$$ Dipole separation

$$b_\perp = \frac{(x_\perp + y_\perp)}{2}$$ Impact parameter

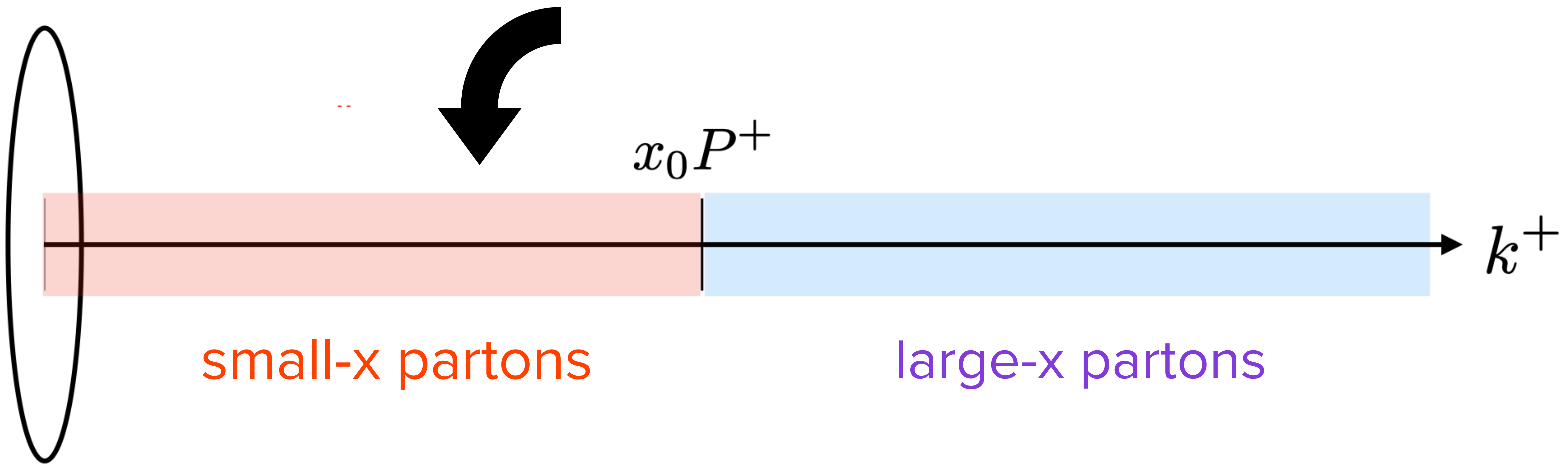

What happens if we probe the observable at $x \ll \boxed{x_0}$?

Momentum fraction at which Weight functional is constructed

Quantum evolution

- Understood as gluon emissions in the interval $[x, x_0]$. Resum large logarithms of $\alpha_s \ln(1/x)$

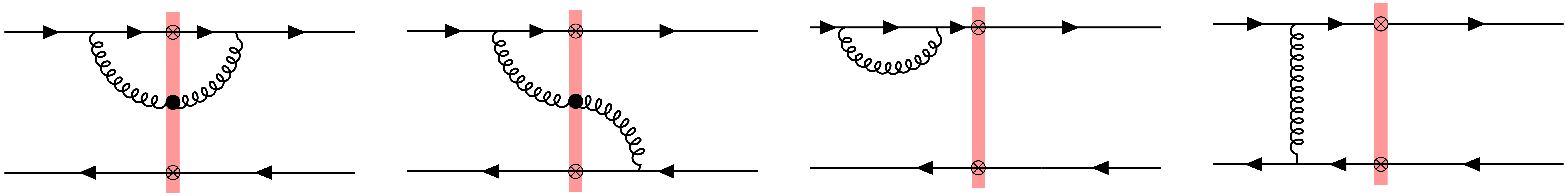

Real diagrams **Virtual diagrams**

- At large N_c , resummation of these terms leads to Balitsky Kochegov (BK) equations

$$\frac{dS^{(2)}_{x_0}(\vec{r}_T)}{d\ln(1/x)} = \frac{\alpha_s N_c}{2\pi^2}\int d^2r'_T \frac{\vec{r}_T^{\,2}}{\vec{r}_T^{\prime 2}(\vec{r}_T - \vec{r}'_T)^2}\left[S^{(2)}_x(r'_T)S^{(2)}_x(|\vec{r}_T - \vec{r}'_T|) - S^{(2)}_x(r_T)\right]$$

Balitsky, Nucl. Phys. B 1996, 463, 99–160,

Kovchegov, Phys. Rev. D 1999, 60, 034008

- The linear and the non-linear term comes from the virtual and real contribution respectively. Weak scattering limit, $D_x(r_T) = 1 - S^{(2)}_x(r_T) \ll 1$: BK equations reduce to BFKL equations

JIMWLK equation

Jalilian-Marian, J.; Kovner, A.; McLerran, L.D.; Weigert, H., Phys. Rev. D 1997, 55, 5414–5428,
Jalilian-Marian, J.; Kovner, A.; Weigert, H., Phys. Rev. D 1998, 59, 014015
Kovner, A.; Milhano, J.G.; Weigert, H., Phys. Rev. D 2000, 62, 114005
Iancu, E.; Leonidov, A.; McLerran, L.D., Nucl. Phys. A 2001, 692, 583–64
Iancu, E.; Leonidov, A.; McLerran, L.D., Phys. Lett. B 2001, 510, 133–144
Ferreiro, E.; Iancu, E.; Leonidov, A.; McLerran, L., Nucl. Phys. A 2002, 703, 489–538

Alternatively, resum the large logarithmic corrections by evolving the weight functional:

$$\frac{dW_x[\rho]}{d\ln(1/x)} = -\mathscr{H}_{\mathrm{JIMWLK}}\, W_x[\rho]$$

Physically, one absorbs the quantum fluctuations in the interval $[x_0 - dx, x_0]$ into stochastic fluctuations of the color sources by redefining the color sources ρ:

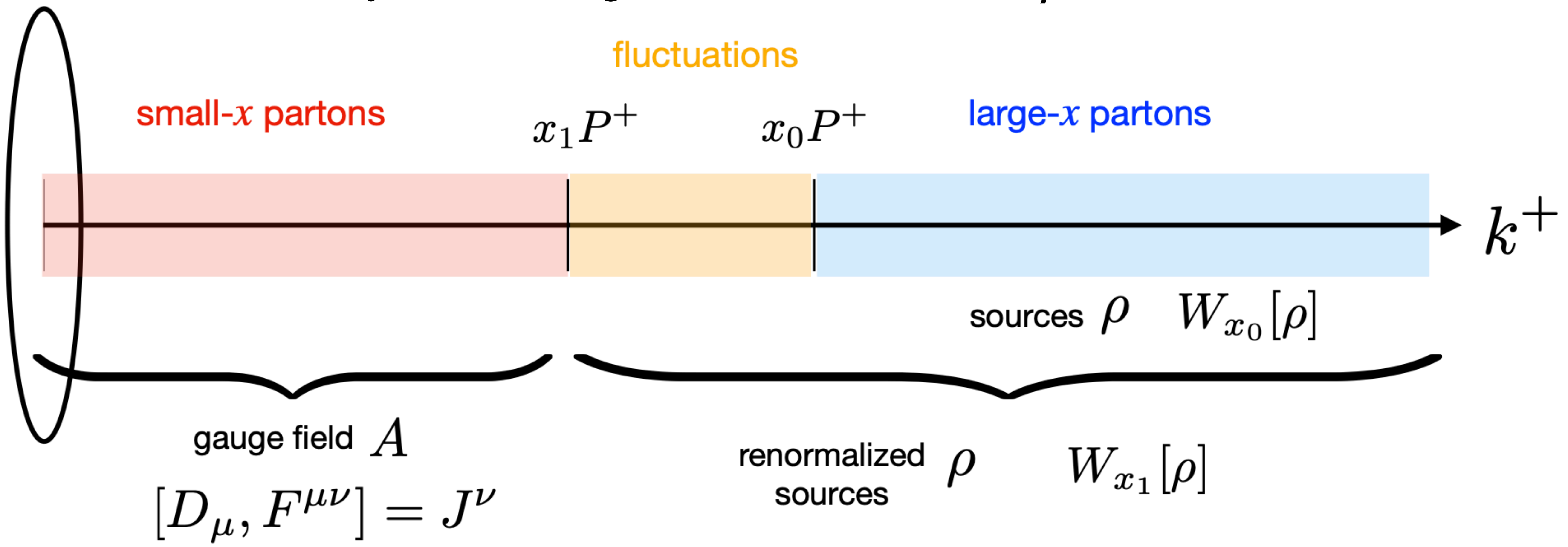

Infrared regulator

Rapidity evolution of Wilson lines in Langevin form

H. Weigert, Nucl. Phys. A 703, 823 (2002)
T. Lappi and H. Mantysaari, Eur. Phys. J. C 73, 2307 (2013)

$$V_{\mathbf{x}}(Y+dY) = \exp\left\{ -i\frac{\sqrt{\alpha_s dY}}{\pi}\int_{\mathbf{z}} \mathbf{K}_{\mathbf{x}-\mathbf{z}}\cdot (V_{\mathbf{z}}\boldsymbol{\xi}_{\mathbf{z}}V_{\mathbf{z}}^\dagger)\right\}$$
$$\times V_{\mathbf{x}}(Y)\exp\left\{ i\frac{\sqrt{\alpha_s dY}}{\pi}\int_{\mathbf{z}} \mathbf{K}_{\mathbf{x}-\mathbf{z}}\cdot \boldsymbol{\xi}_{\mathbf{z}}\right\},$$

ξ is Gaussian noise with zero average

The JIMWLK Kernel is modified to avoid infrared tails:

$$\mathbf{K}_{\mathbf{r}}^{(\mathrm{mod})} = m|\mathbf{r}|\ K_1(m|\mathbf{r}|)\ \mathbf{K}_{\mathbf{r}}$$

B. Schenke, S. Schlichting Phys.Lett.B 739 (2014) 313-319

JIMWLK evolution on dipole amplitude

The quantum evolution effectively increases the color charge density, and hence Q_s

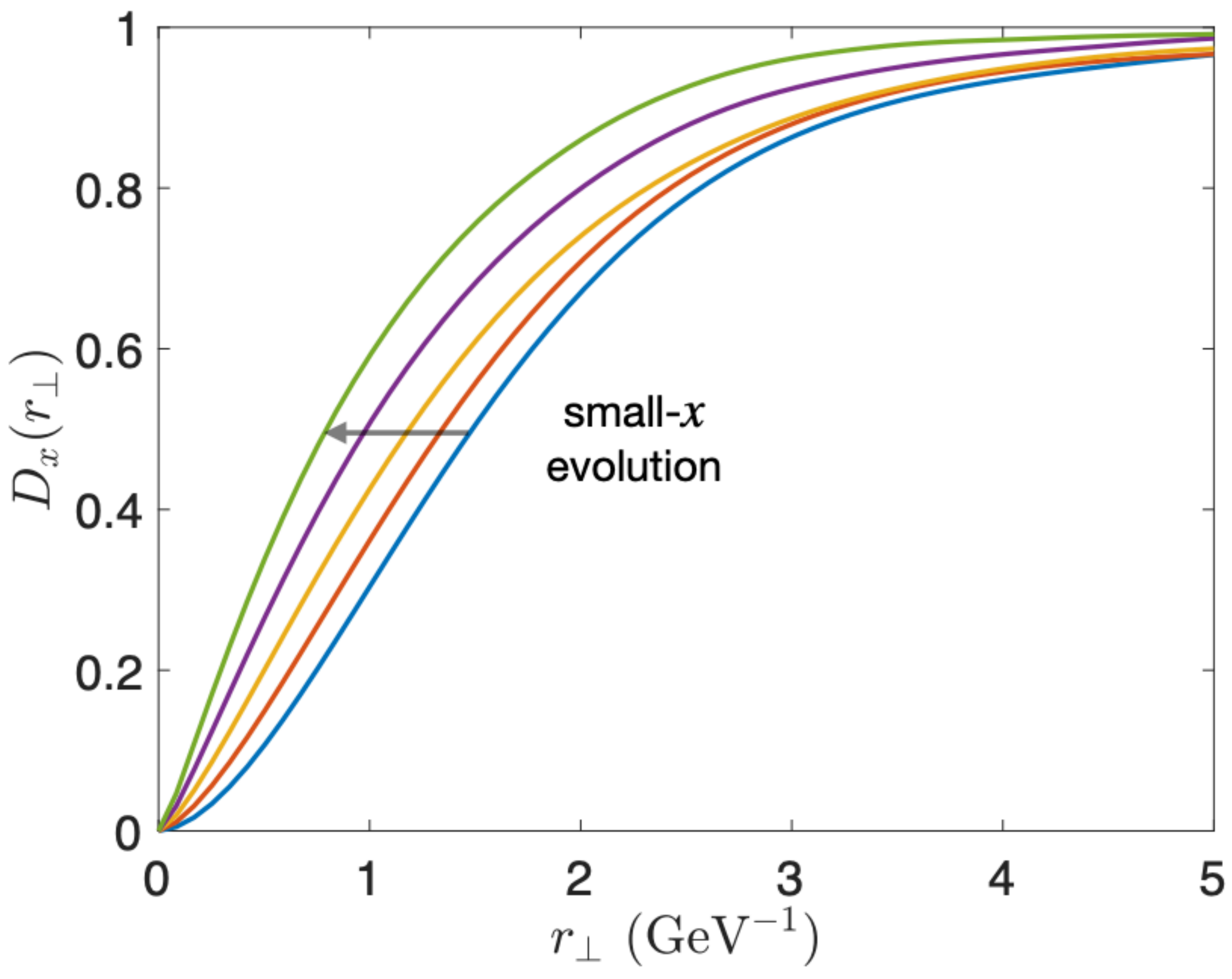

Small dipole $r_\perp \leq 1/Q_s$ scatter very little

Large dipole $r_\perp \geq 1/Q_s$ scatter with probability 1

Effect on the dipole amplitude $D_x(r_T) = 1 - S_x^{(2)}(r_T)$

Color Glass Condensate revisited

- Structure at small-x characterised by the correlation function of Wilson lines
- Based on high-energy factorization, single inclusive observables (like multiplicity) can be calculated to leading log. (LL) accuracy as an average over color charge distributions inside projectile and target

F Gelis, T Lappi, R Venugopalan, PRD 78, 054019 (2008), PRD 78, 054020 (2008), PRD 79, 094017 (2008)

$$\left.\frac{dN}{dy}\right|_{y_{\rm obs}} = \int [DU][DV]\; \mathcal{W}^{p}_{y_{\rm obs}-y_{\rm p}}[U]\mathcal{W}^{t}_{y_{\rm obs}-y_{\rm t}}[U]\;\frac{dN}{dy}[U,V]$$

rapidity separation between projectile and measured rapidity

rapidity separation between target and measured rapidity

- Evolution of weight-functionals $W_{\Delta y}$ with the rapidity separation Δy is described by JIMWLK evolution equation

Beyond boost invariance

- Boost invariance (η~0) on average is reasonable assumption for symmetric high-energy collisions

- New measurements at RHIC and LHC indicates towards the presence of **longitudinal dynamics**

  Event plane decorrelation Phys.Rev.C 92 (2015) 3, 034911,...

  Flow decorrelation Eur. Phys. J. C 76 (2018) 142, …

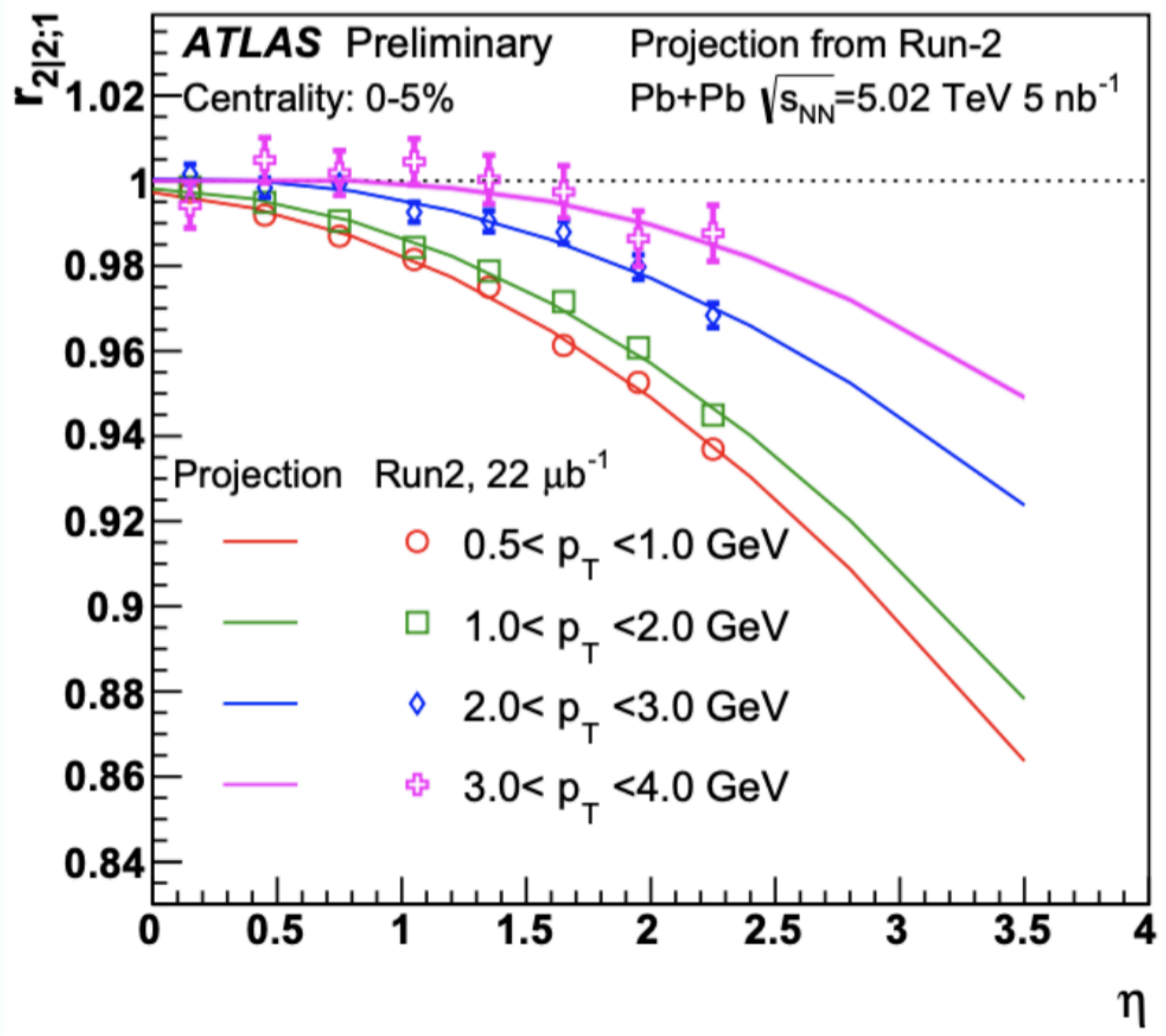

- Available 3+1D frameworks:

  Generalisation of 2+1D CGC model Phys.Rev.C 94 (2016) 4, 044907, Nucl.Phys.A 1005 (2021), 121771, …

  Phenomenological model Phys.Lett.B 752 (2016), 206-211, Phys.Lett.B 752 (2016), 317-321, ...

  3D CGC (Coloured particle in cell method) Phys.Rev.D 94 (2016) 1, 014020

  3+1 D Classical Yang-Mills simulation (CYM) Phys.Rev.D 103 (2021) 1, 014003

3+1D IP-Glasma model (Classical Yang-Mills + QCD JIMWLK evolution)

B. Schenke, S. Schlichting, PRC94, 044907 (2016)

- Generate configuration of Wilson lines U,V at initial rapidity separation y_{init} based on IP-Sat

  IP-Sat model → provides the Q_s by fitting the dipole cross section to HERA data

- Evolve Wilson lines U,V from initial rapidity y_{init} to all rapidities y_{obs} of interest s.t $y_{\text{obs}} > y_{\text{init}}$

- Compute observables at all rapidities of interest by solving classical Yang-Mills equations

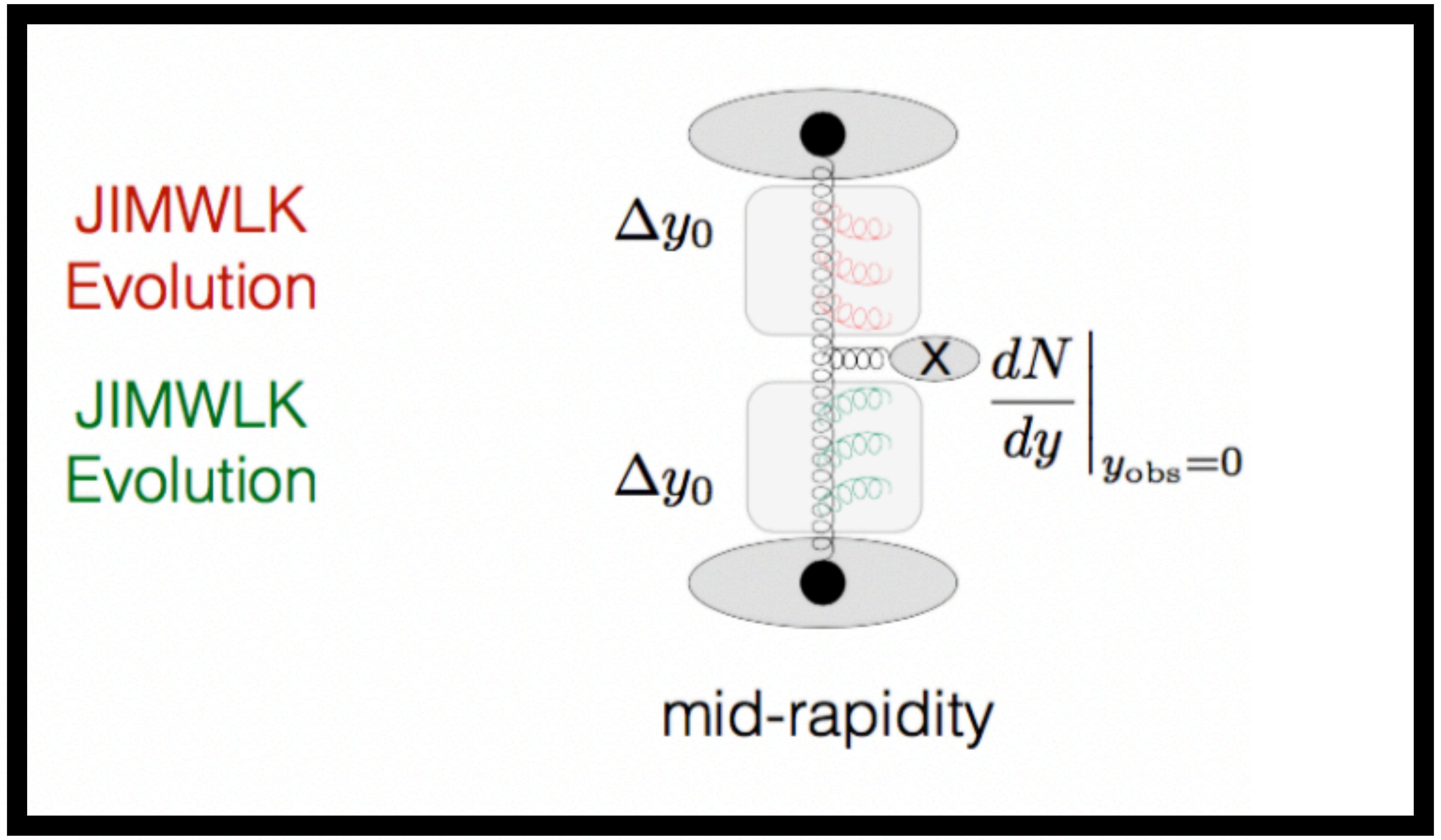

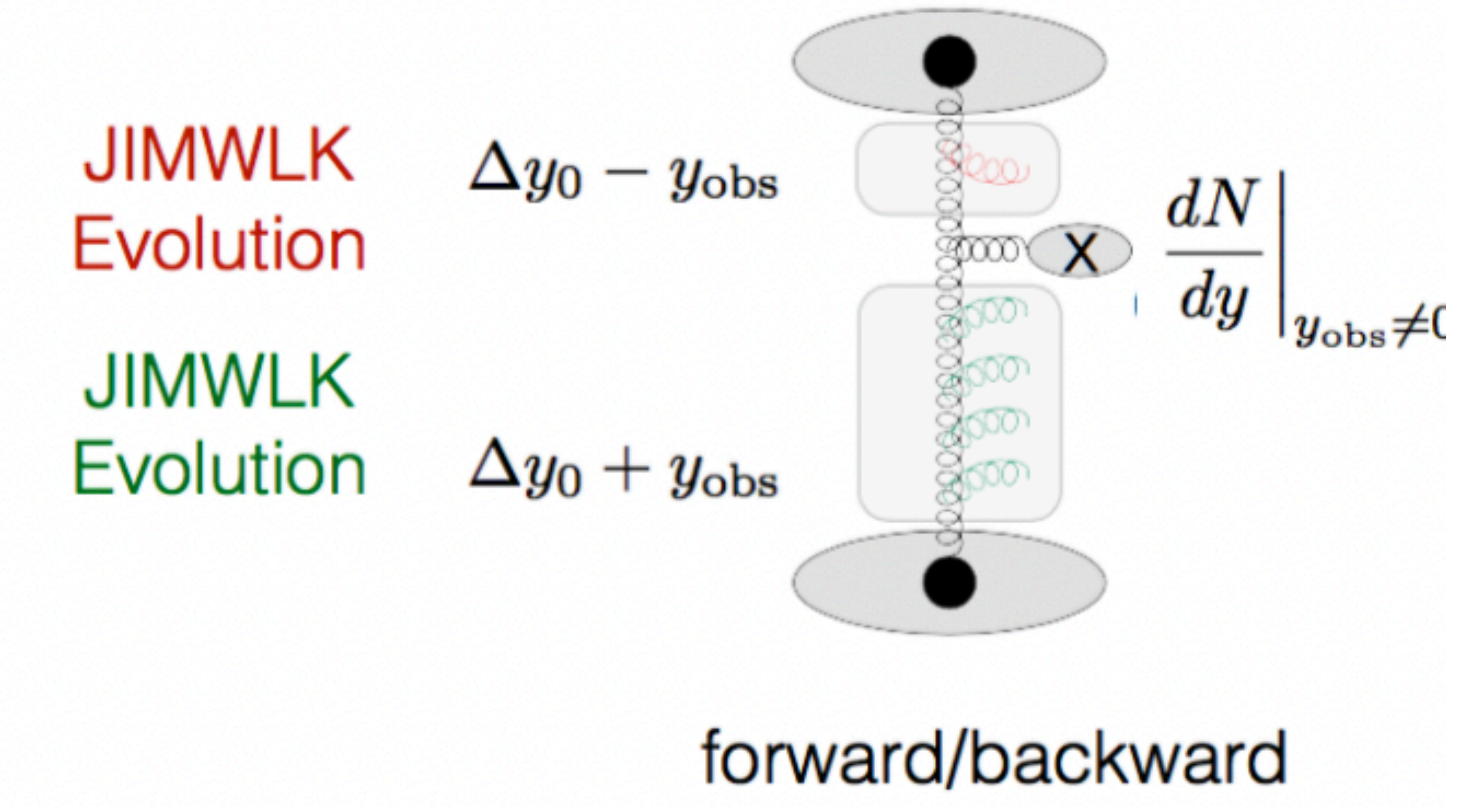

Color charge densities of the incoming nuclei

- Sample nucleon positions using some distributions (Wood-Saxon here)
- Use IP-Sat model fit to HERA data to get $Q_s^2(x, b_\perp)$ for each nucleon. The color charge density squared $g^2\mu^2$ is proportional to Q_s^2
- Obtain $g^2\mu^2(x_\perp)$ for each nucleus by summing corresponding quantities $g^2\mu^2(x, b_\perp, x_\perp)$ of all individual nucleons

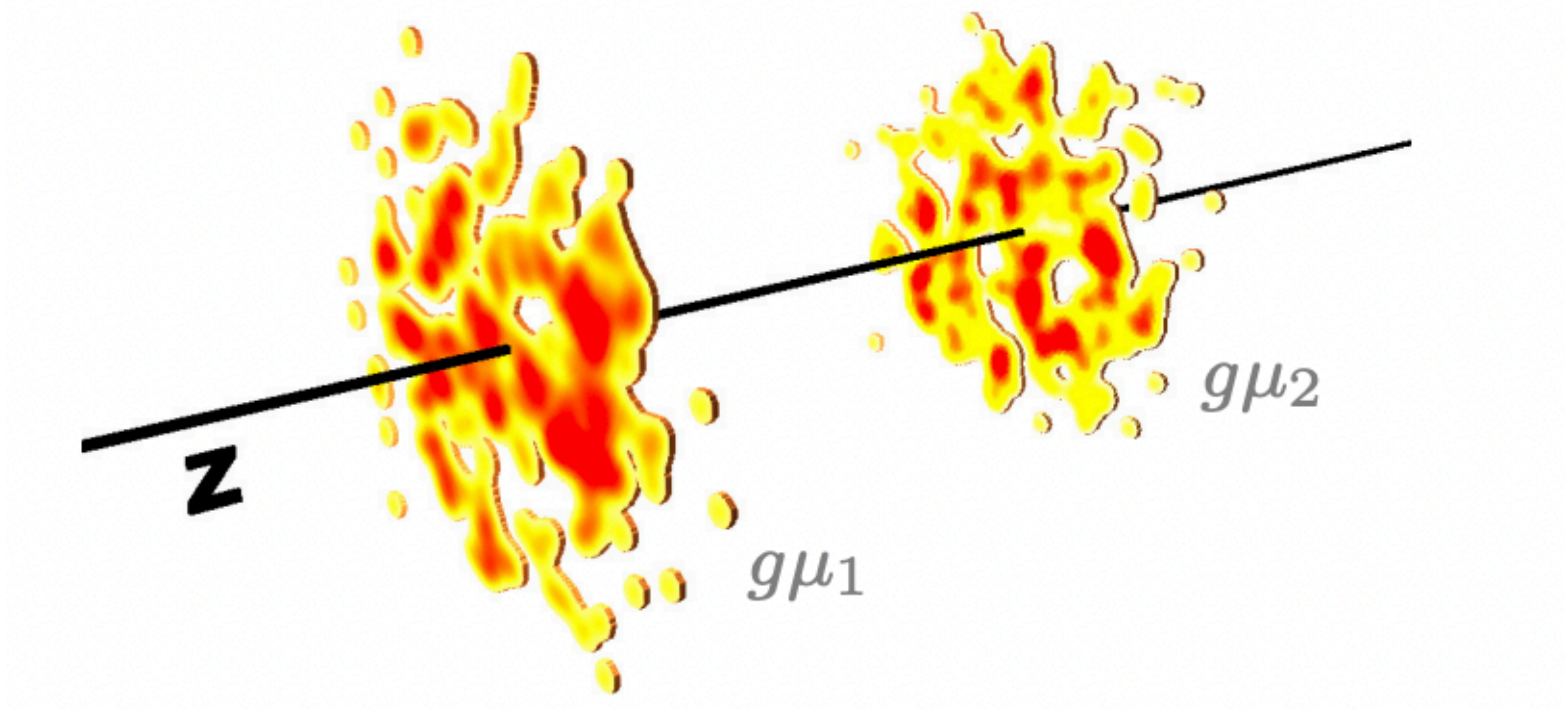

- Sample ρ^a from local Gaussian distribution for each nucleus

$$\langle \rho^a(\mathbf{x}_\perp)\rho^b(\mathbf{y}_\perp)\rangle = \delta^{ab}\delta^2(\mathbf{x}_\perp - \mathbf{y}_\perp)g^2\mu^2(\mathbf{x}_\perp)$$

JIMWLK evolution of a Pb nucleus

B. Schenke, S. Schlichting, PRC94, 044907 (2016)

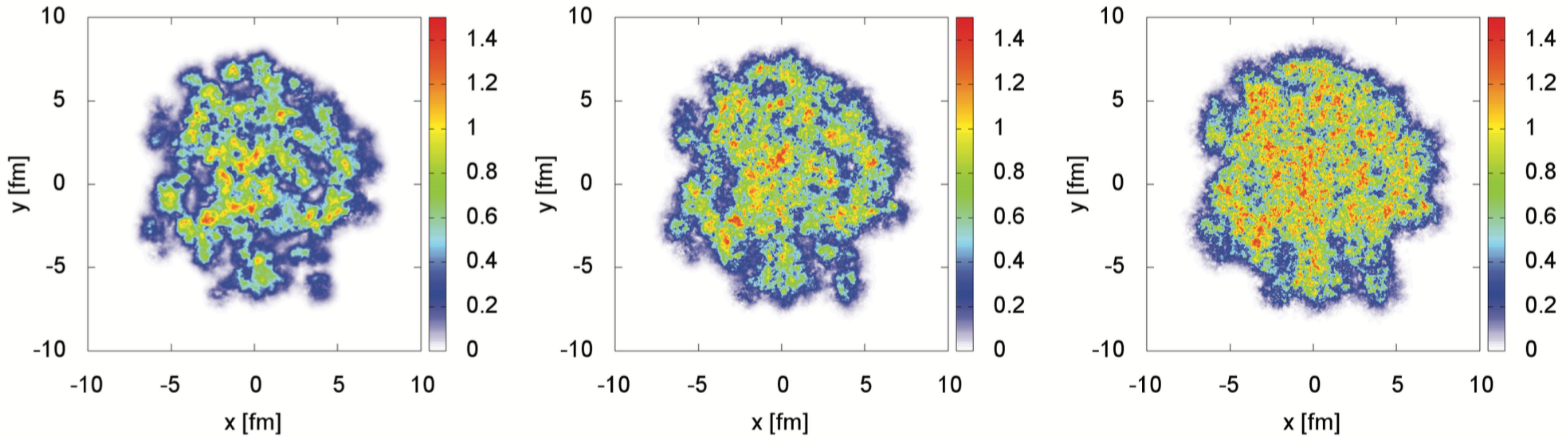

Y = −2.4 (x ≈ 2×10^{-3})   Y = 0 (x ≈ 2×10^{-4})   Y = 2.4 (x ≈ 1.6×10^{-5})

FIG. 2. JIMWLK evolution of the gluon fields in one nucleus for $m = 0.4\,\mathrm{GeV}$ and $\alpha_s = 0.3$. Shown is $1 - \mathrm{Re}[\mathrm{tr}(V_{\mathbf{x}})]/N_c$ in the transverse plane at rapidities $Y = -2.4$ ($x \approx 2 \times 10^{-3}$) (a), $Y = 0$ ($x \approx 2 \times 10^{-4}$) (b), and $Y = 2.4$ ($x \approx 1.6 \times 10^{-5}$) (c) to illustrate the change of the typical transverse length scale with decreasing x. The global geometry clearly remains correlated over the entire range in rapidity.

Small scale fluctuations develop and become finer and finer as characterized by the growth of Q_s

Modification of nuclear profile in Pb nucleus

H. Mäntysaari, F. Salazar, B. Schenke, arXiv:2207.03712

Extract nuclear profile from γ + Pb → J/ψ + Pb |t| spectra in UPC collisions

$$T_A(b) \propto \int \Delta\, \mathrm{d}\Delta\, J_0(b\Delta)(-1)^n \sqrt{\frac{\mathrm{d}\sigma^{\gamma^*+\mathrm{Pb}\to \mathrm{J}/\psi+\mathrm{Pb}}}{\mathrm{d}|t|}},$$

$$\int \mathrm{d}^2 b\, T_A(b) = 208.$$

The uncertainty band is obtained by varying the upper limit of the |t| integration between 0.07 …0.1GeV^2 and the number of nuclear color charge configurations used to calculate coherent J/ψ production cross section.

$x = 10^{-2} \to 10^{-4} \to 10^{-5}$

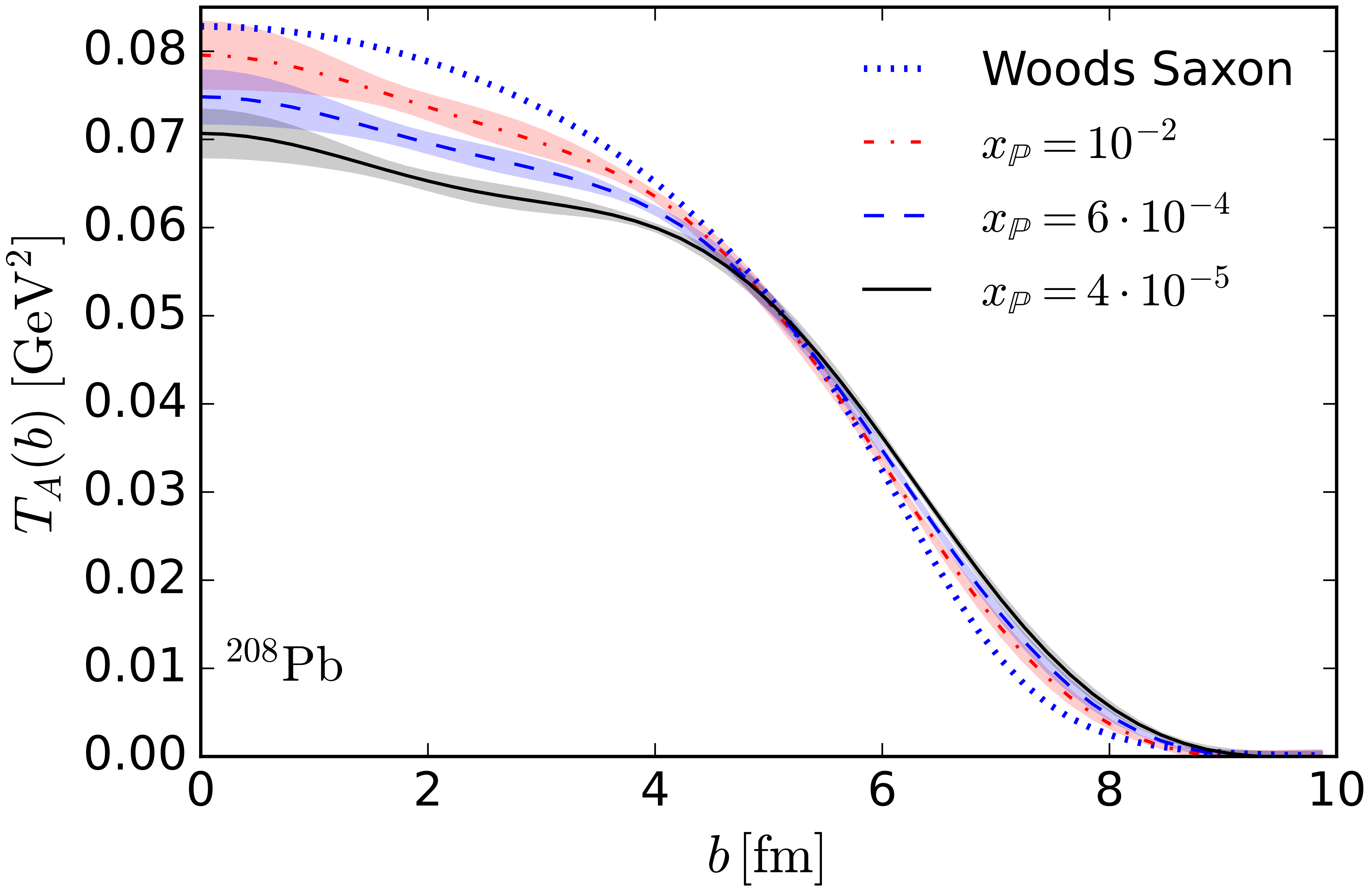

Effect of JIMWLK evolution on deformation

Using a fictitious nucleus like U but with $\beta_2 = 0.8$

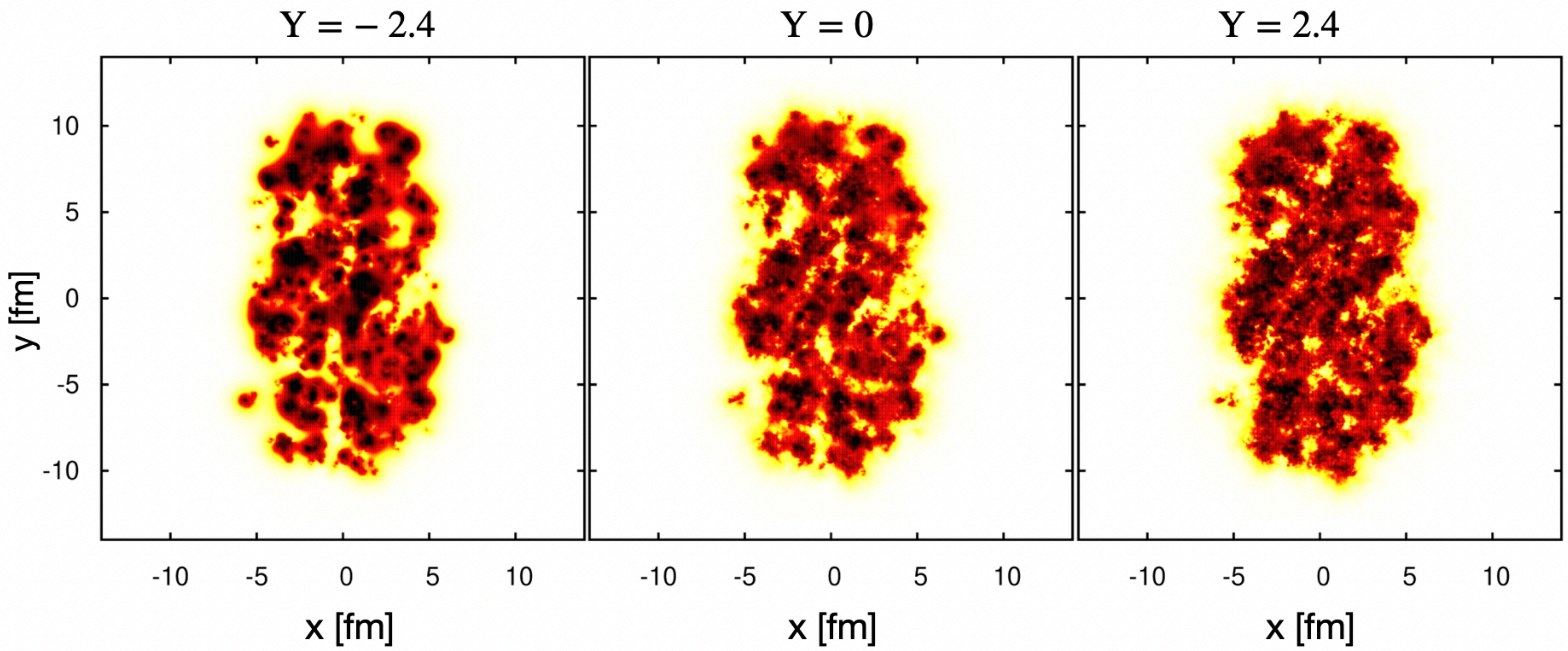

Eccentricity in b=0 collisions

Using U with $\beta_2 = 0.28$

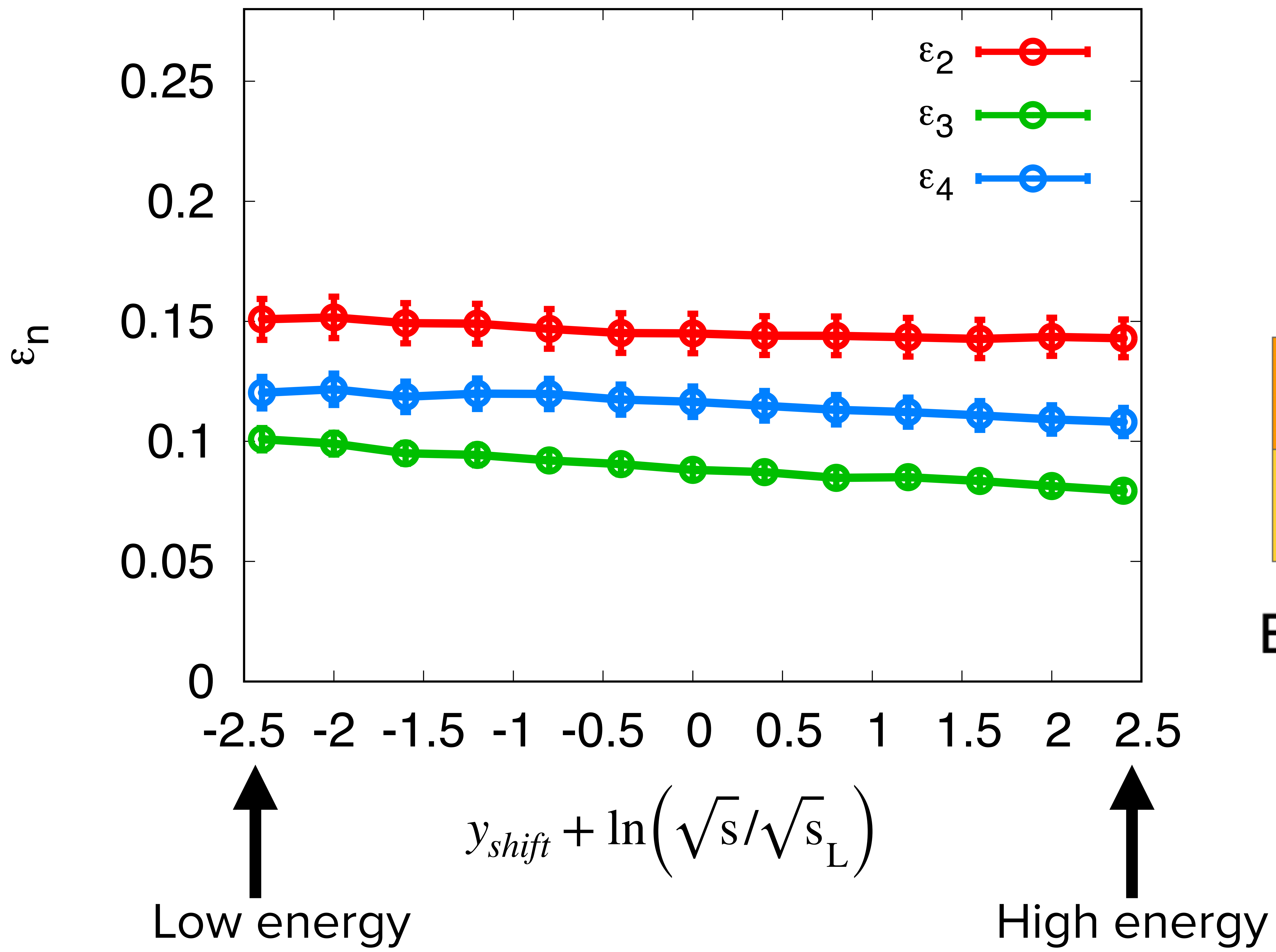

Same amount of rapidity evolution has been done for both the nuclei to compute observables at mid-rapidity

$$\varepsilon_n(y) = \frac{\int d^2\mathbf{r}_\perp T^{\tau\tau}(y,\mathbf{r}_\perp)\ |\mathbf{r}_\perp|^n e^{in\phi_{\mathbf{r}_\perp}}}{\int d^2\mathbf{r}_\perp T^{\tau\tau}(y,\mathbf{r}_\perp)\ |\mathbf{r}_\perp|^n},$$

	ϵ_2	ϵ_3	ϵ_4
Ratio $y_{2.4}/y_{-2.4}$	0.948	0.788	0.897

Eccentricity ratio of evolved to non-evolved

Effect of JIMWLK evolution on small systems

Ne-20, a strongly correlated system

$Y = 0$

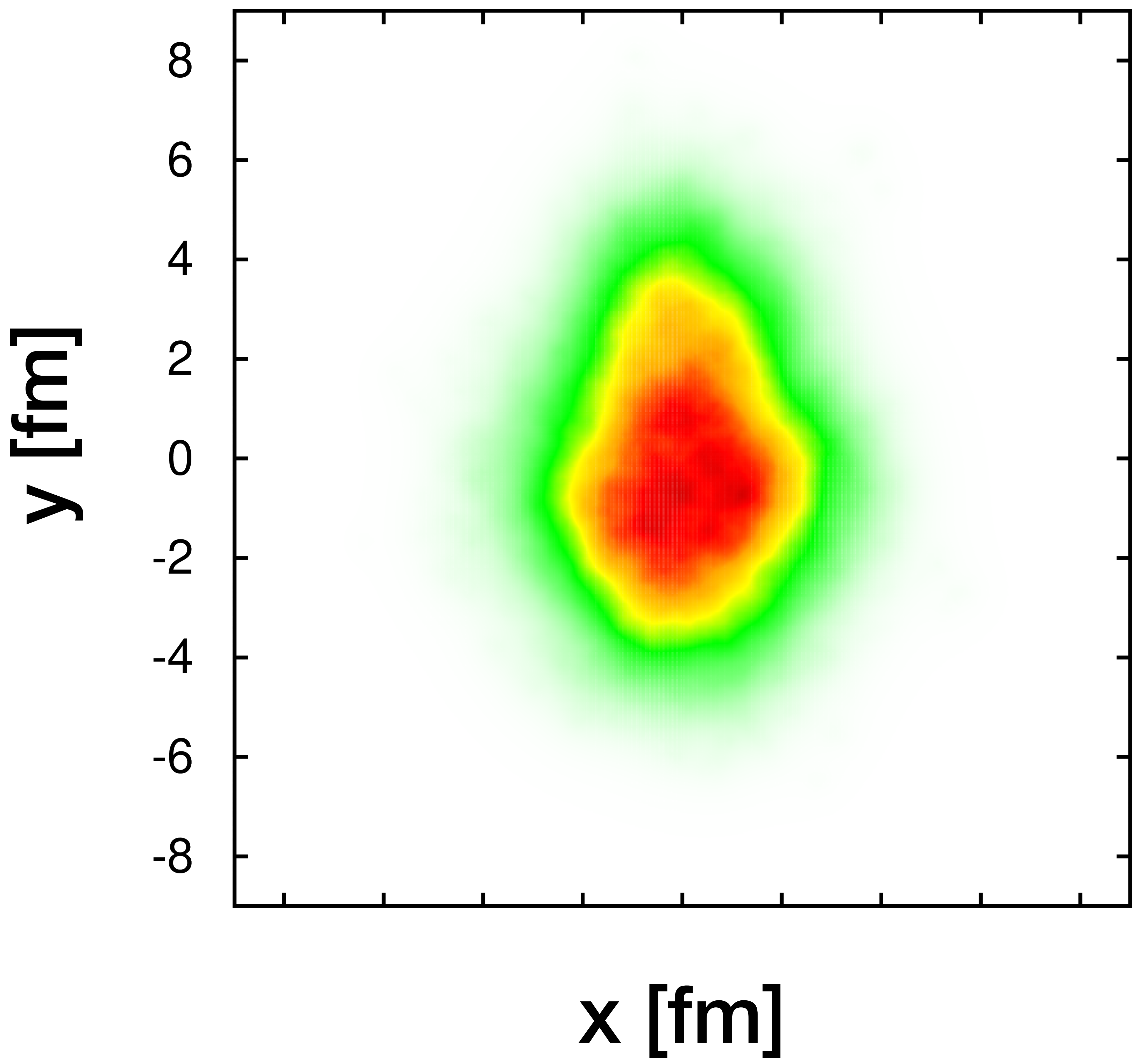

$Y = 4.6$

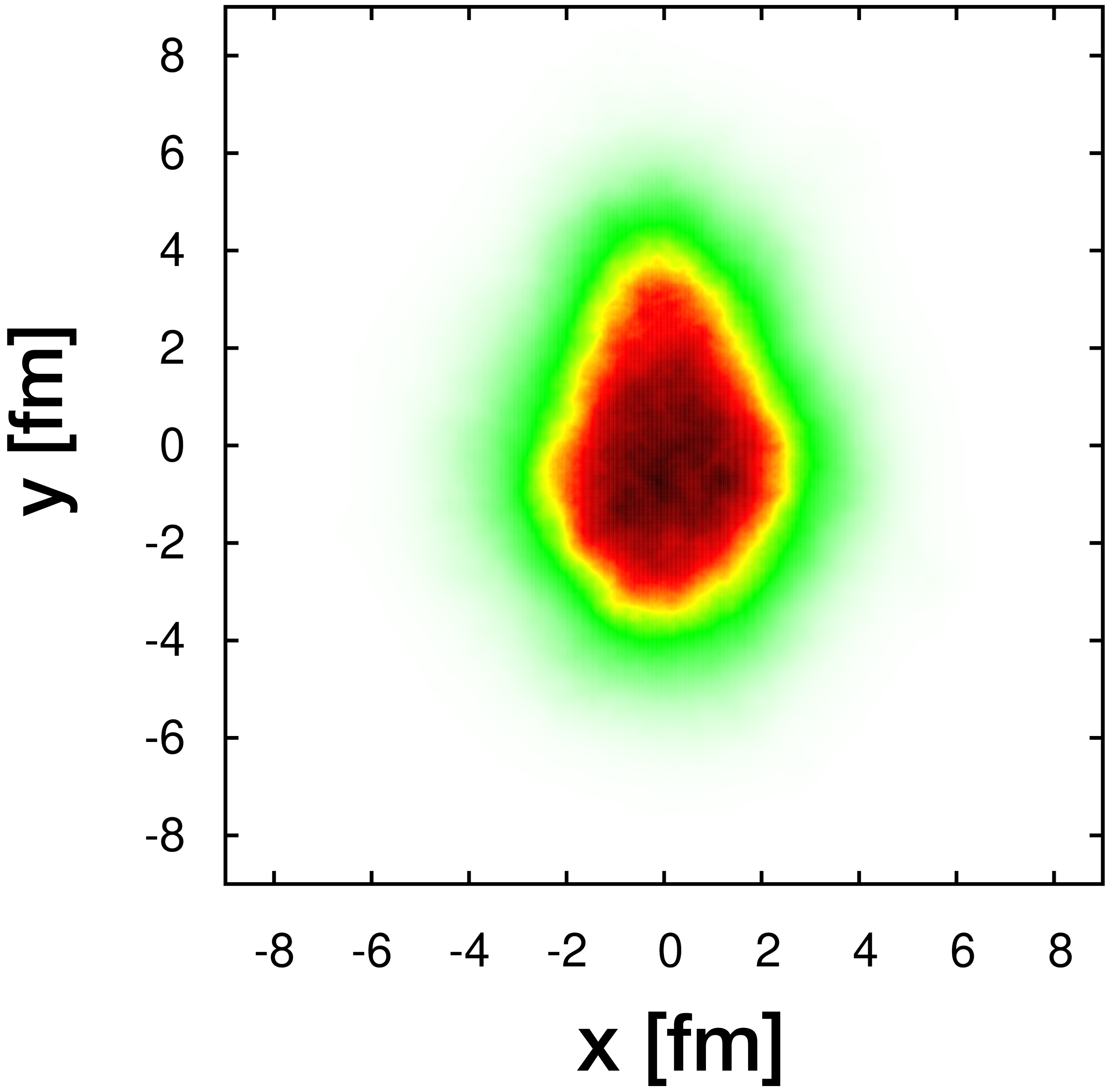

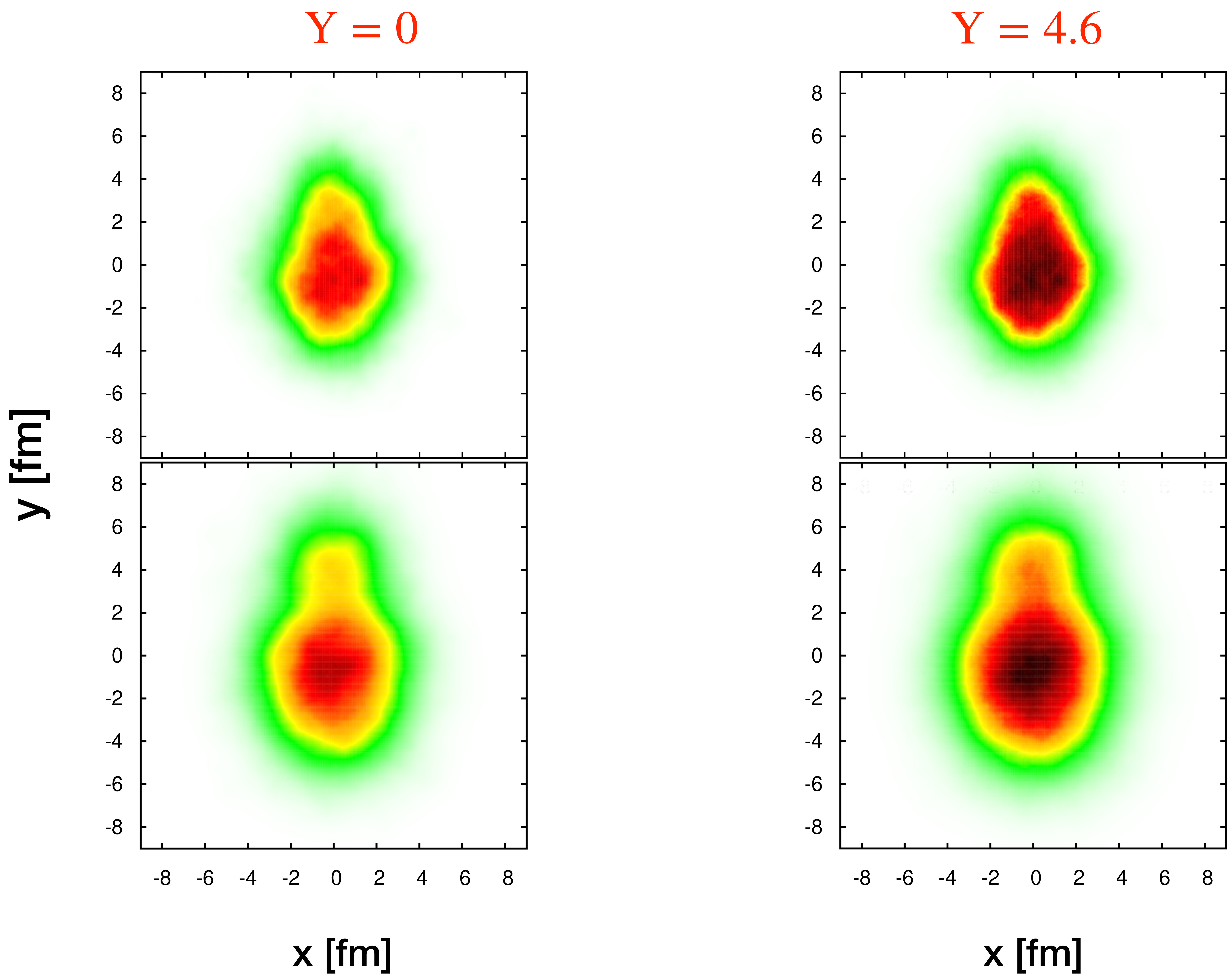

Wood-Saxon (WS)

Projected Generator Coordinate Method (PGCM)

Effect of JIMWLK evolution on small systems

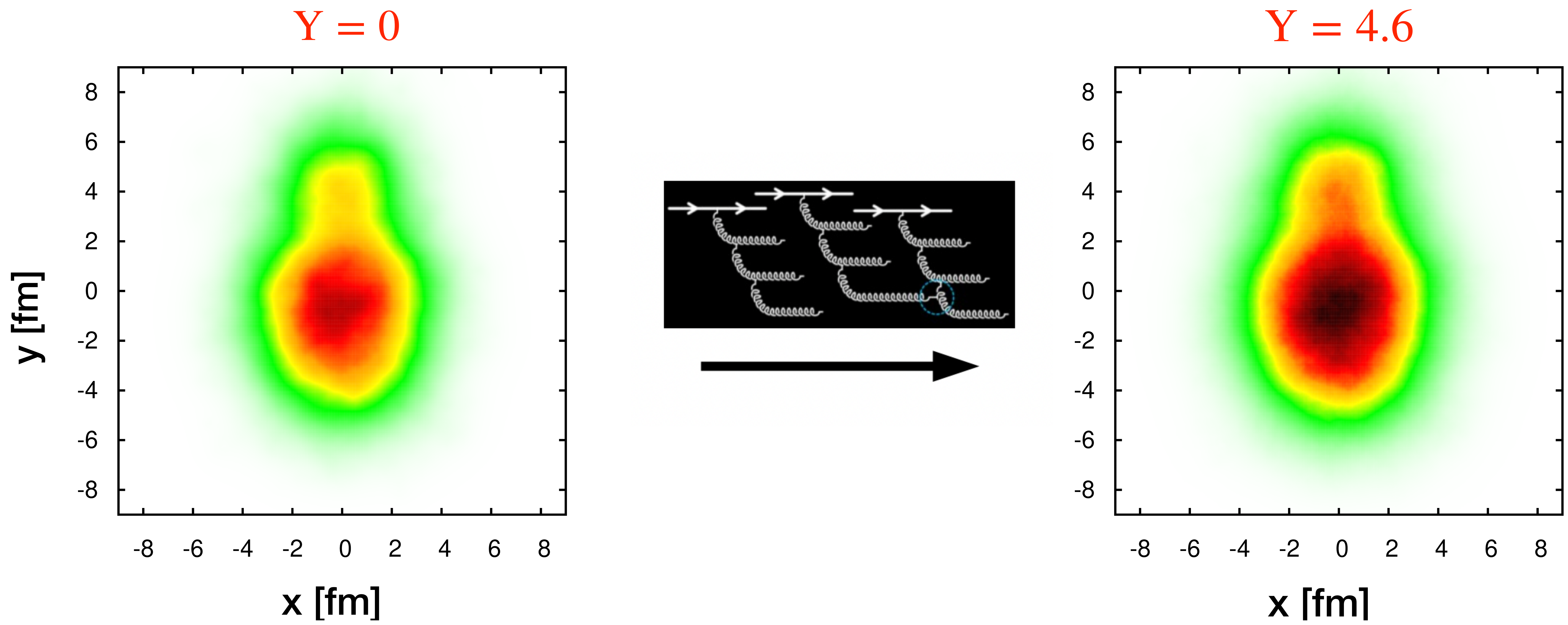

Small-x evolution does not melt the bowling pin shape

Eccentricities for Ne-20 at b=0 fm

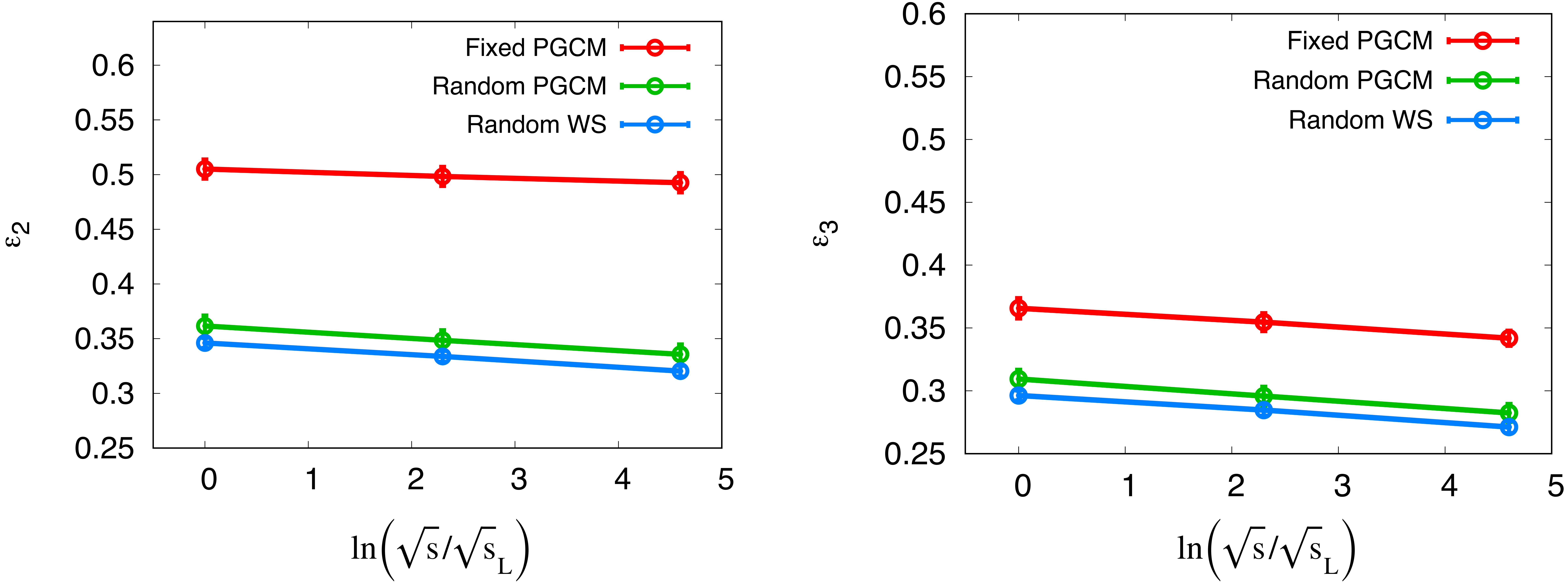

Azimuthal anisotropy of produced gluons

$$\boxed{Q_s^2 \sim (A/x)^{1/3}}$$

For U-U and Ne-Ne collisions at b=0 fm

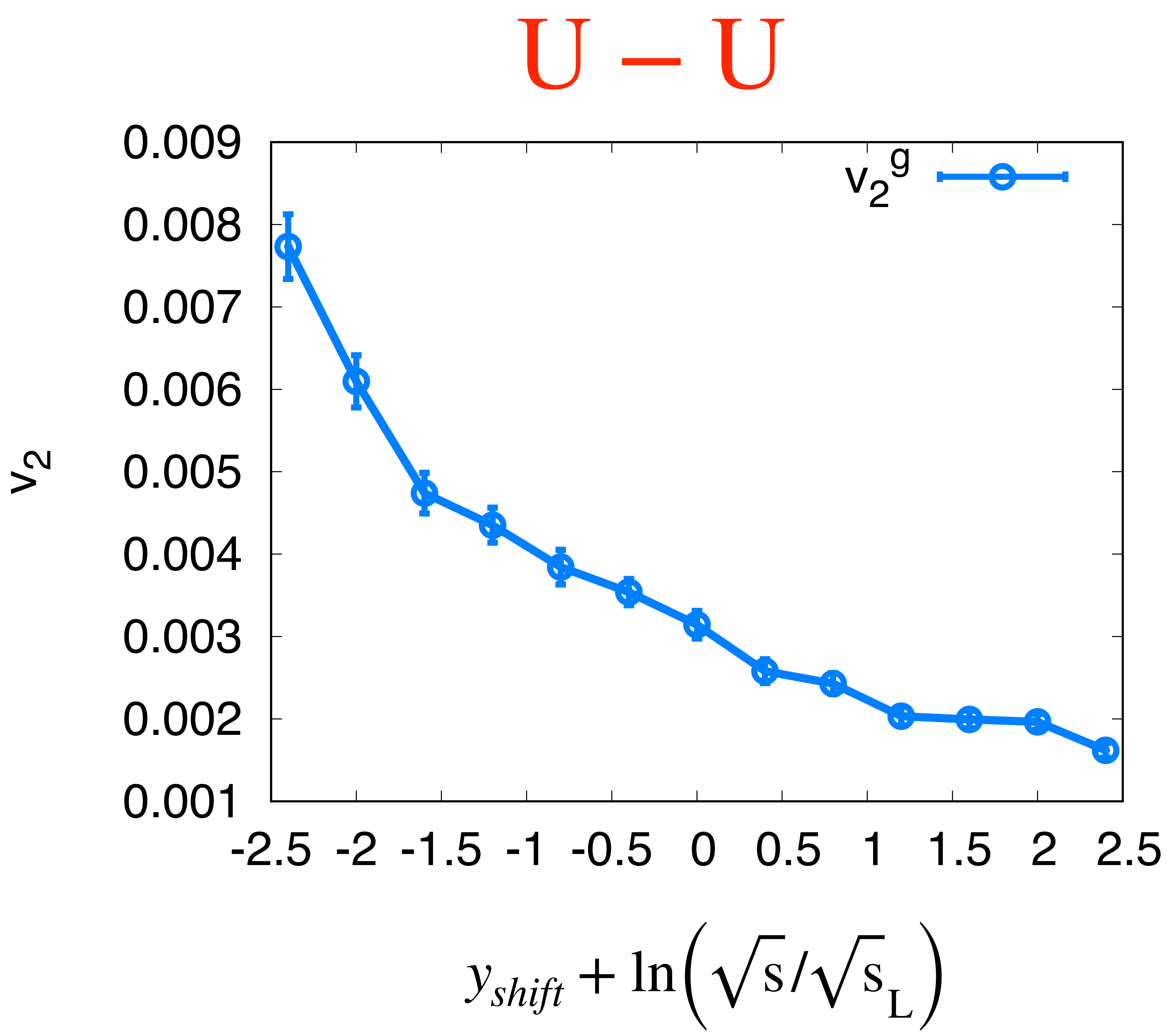

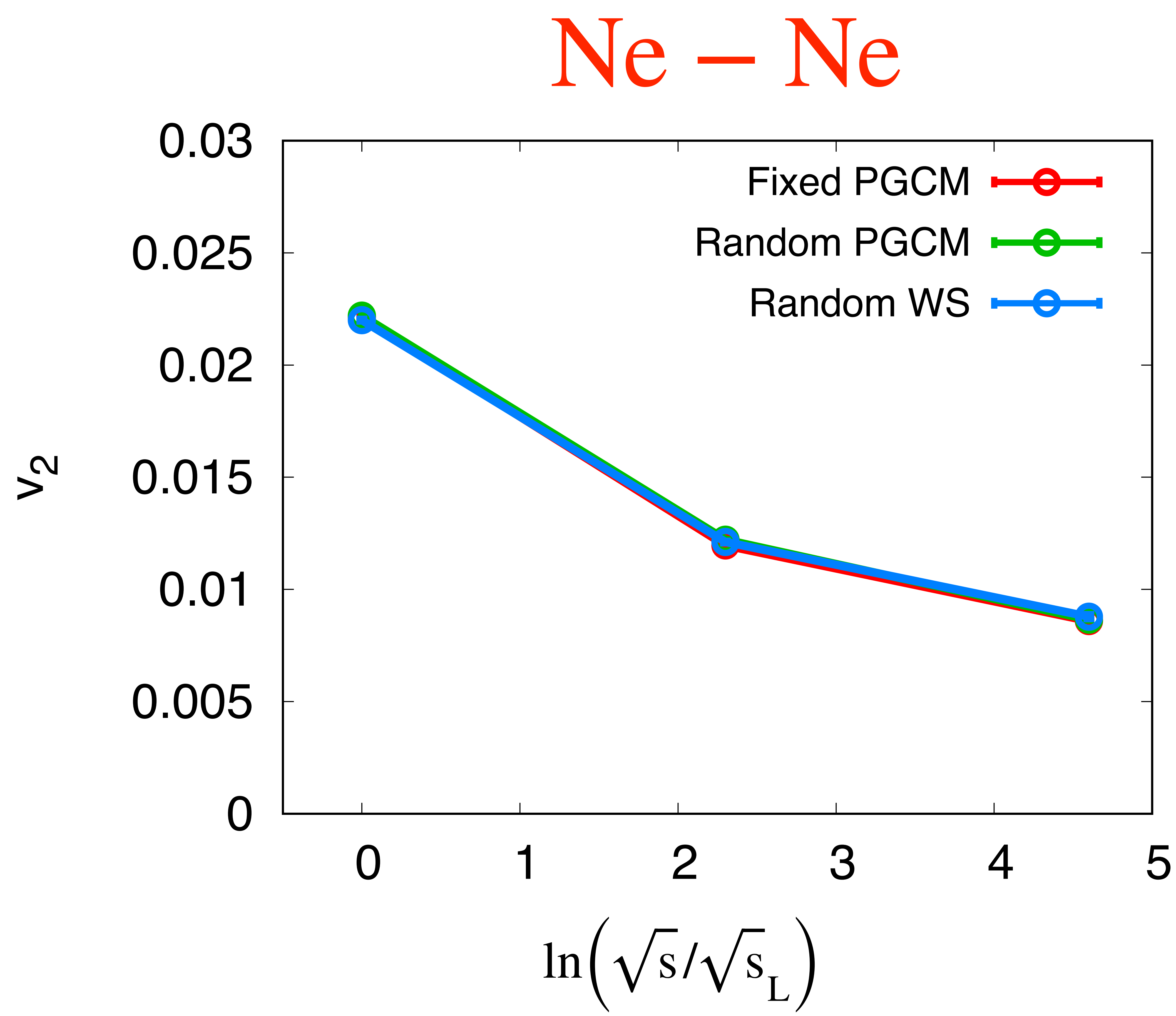

Rho estimator : Distinguish the source of anisotropy

P. Bozek, Phys. Rev. C 93. 044908 (2016),
B. Schenke, C. Shen, D. Teaney, Phys. Rev. C 102, 034905 (2020)
G. Giacalone, B. Schenke, C. Shen, Phys. Rev. Lett. 125 (2020) 19, 192301

Use the correlation of mean transverse momentum $[p_T]$ and v_2^2 at fixed multiplicity.

$$\hat{\rho}(v_2^2, [p_T]) = \frac{\langle \hat{\delta} v_2^2\, \hat{\delta}[p_T] \rangle}{\sqrt{\langle (\hat{\delta} v_2^2)^2 \rangle \langle (\hat{\delta}[p_T])^2 \rangle}}$$

$$\delta O = O - \langle O \rangle$$

$$\hat{\delta} O \equiv \delta O - \frac{\langle \delta O \delta N \rangle}{\sigma_N^2} \delta N$$

A. Olszewski, W. Broniewski, Phys. Rev. C96, 054903 (2017)

The two origins of v_2 have very distinct predictions for this correlator.

Rho estimator for Ne-20 at b=0 fm

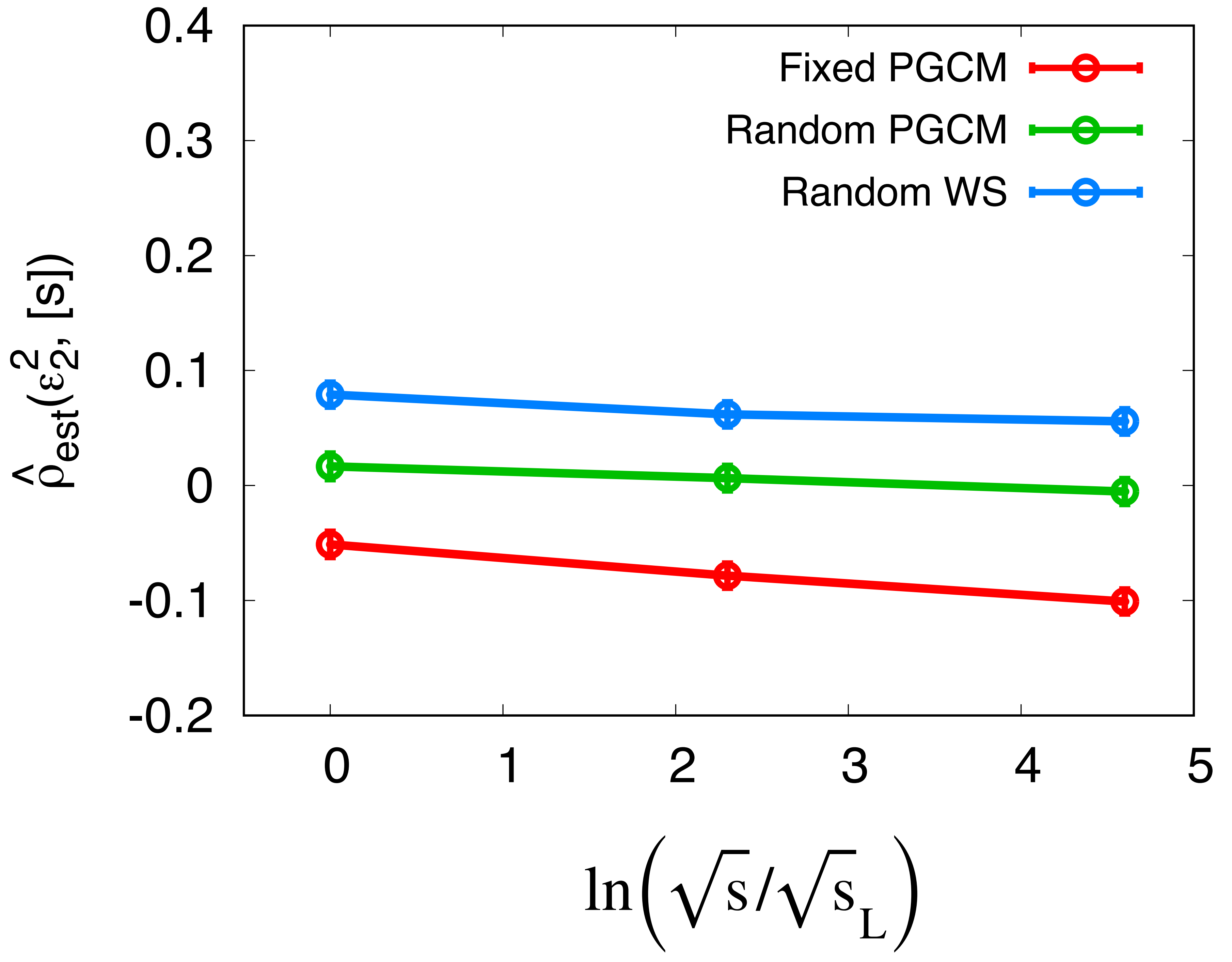

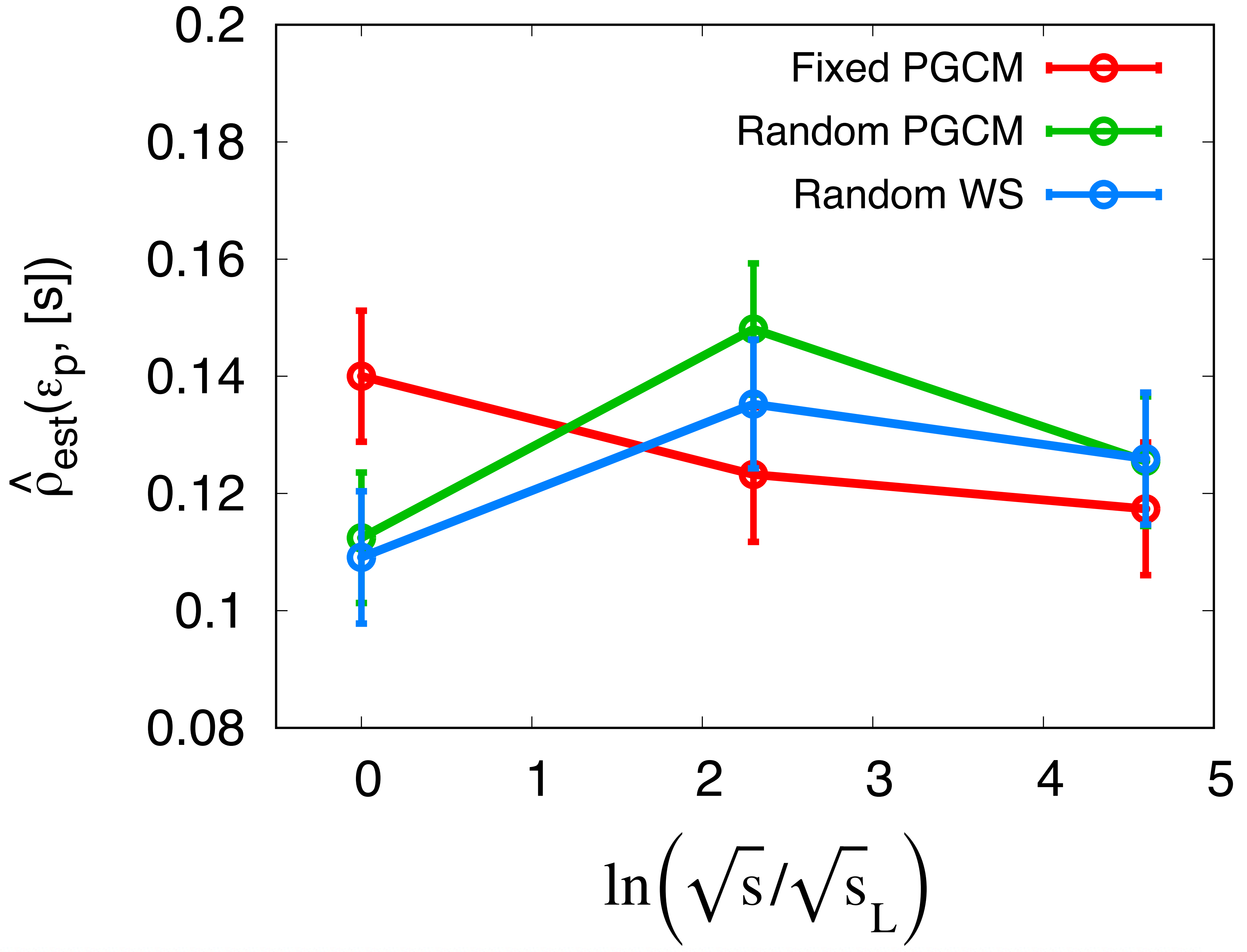

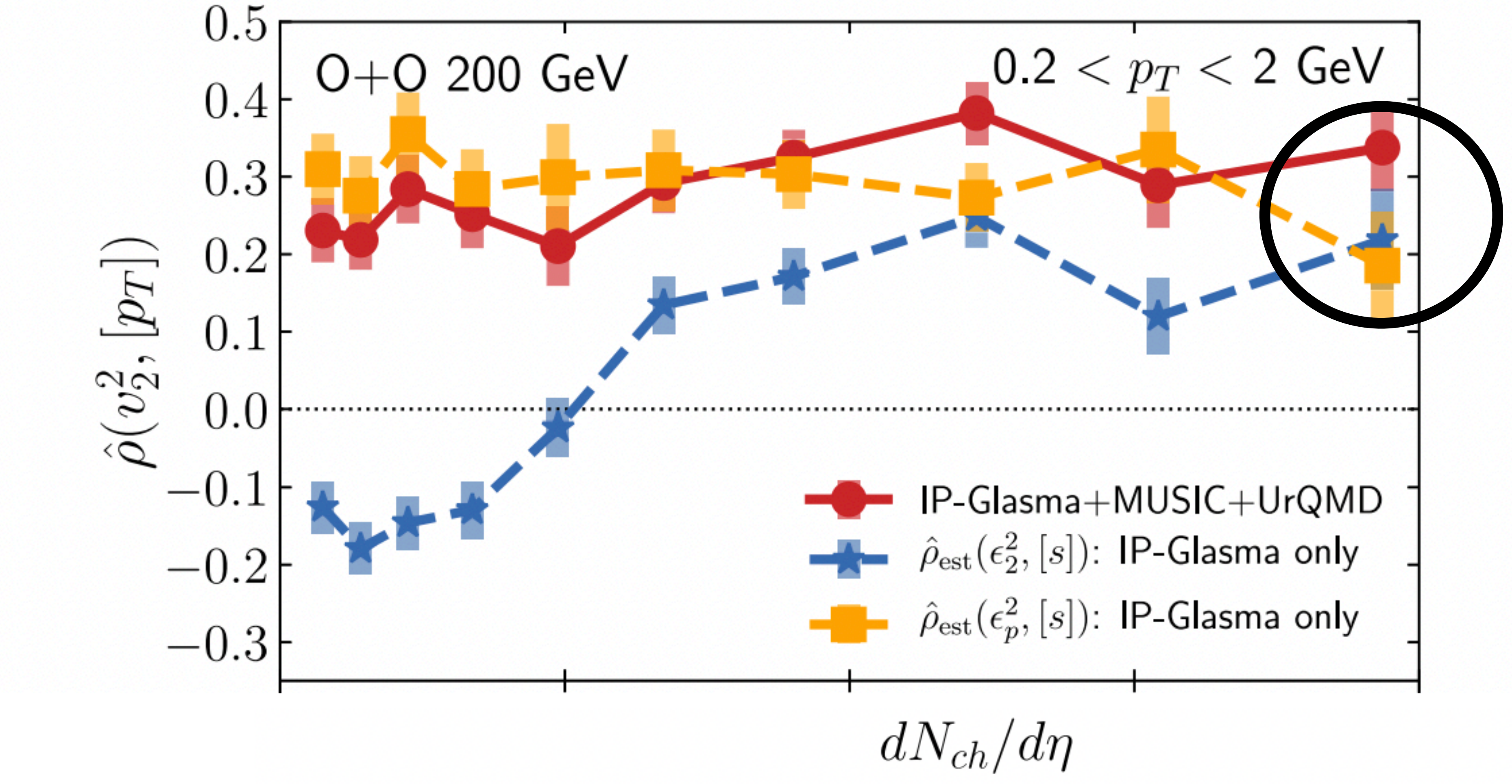

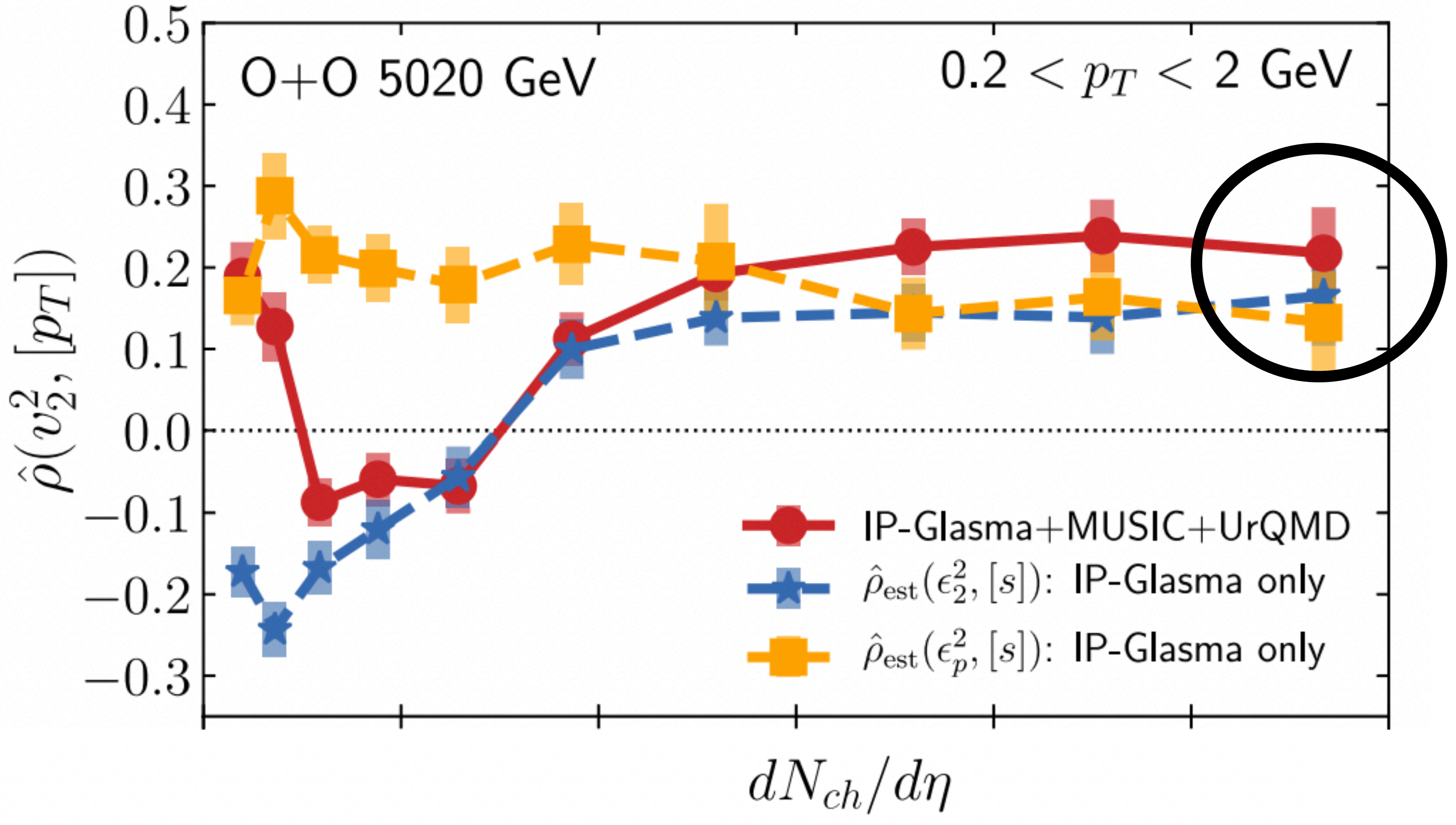

Effect of JIMWLK evolution on Ru (Case 1)

R_p [fm]	σ_p [fm]	R_n [fm]	σ_n [fm]	β_2	β_3
5.085	0.46	5.085	0.46	0.158	0

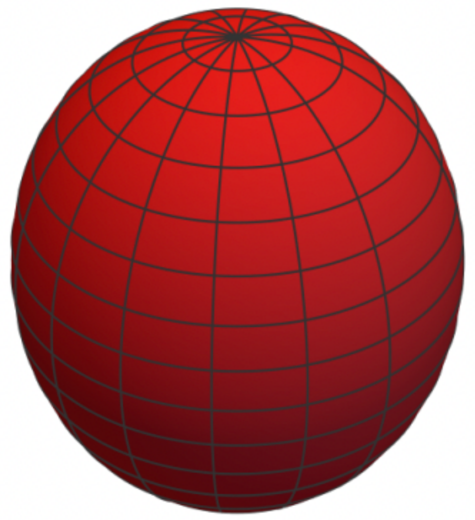

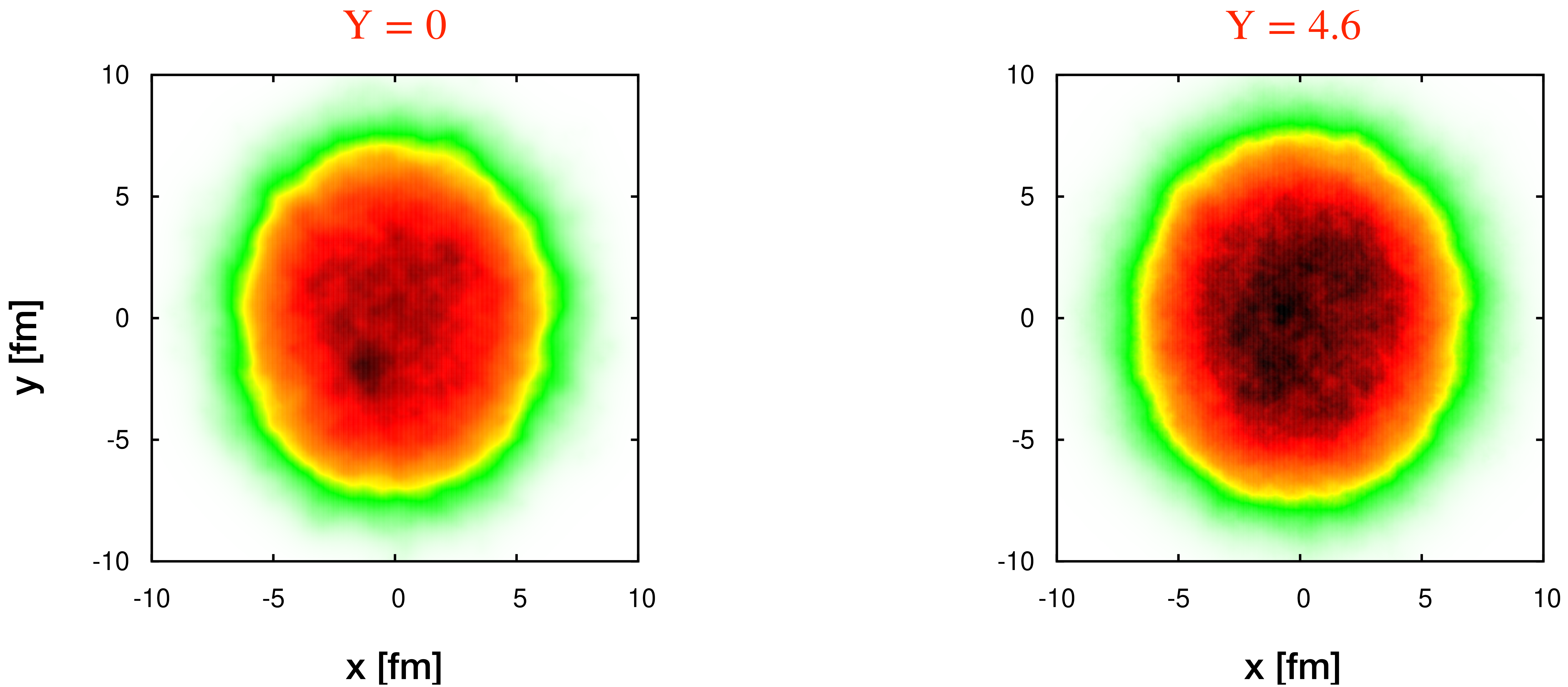

Effect of JIMWLK evolution on Zr (Case 5)

R_p [fm]	σ_p [fm]	R_n [fm]	σ_n [fm]	β_2	β_3
4.912	0.508	5.007	0.564	0.062	0.202

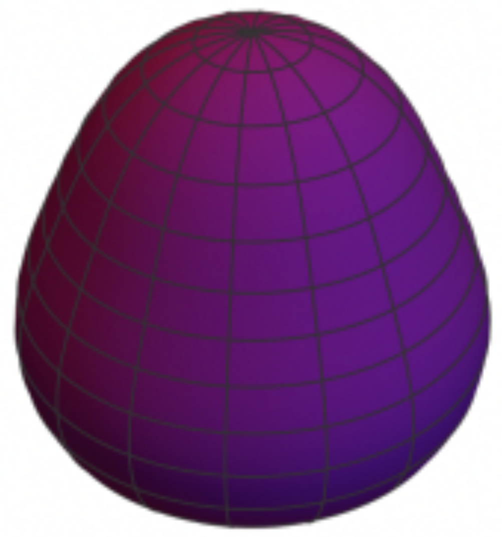

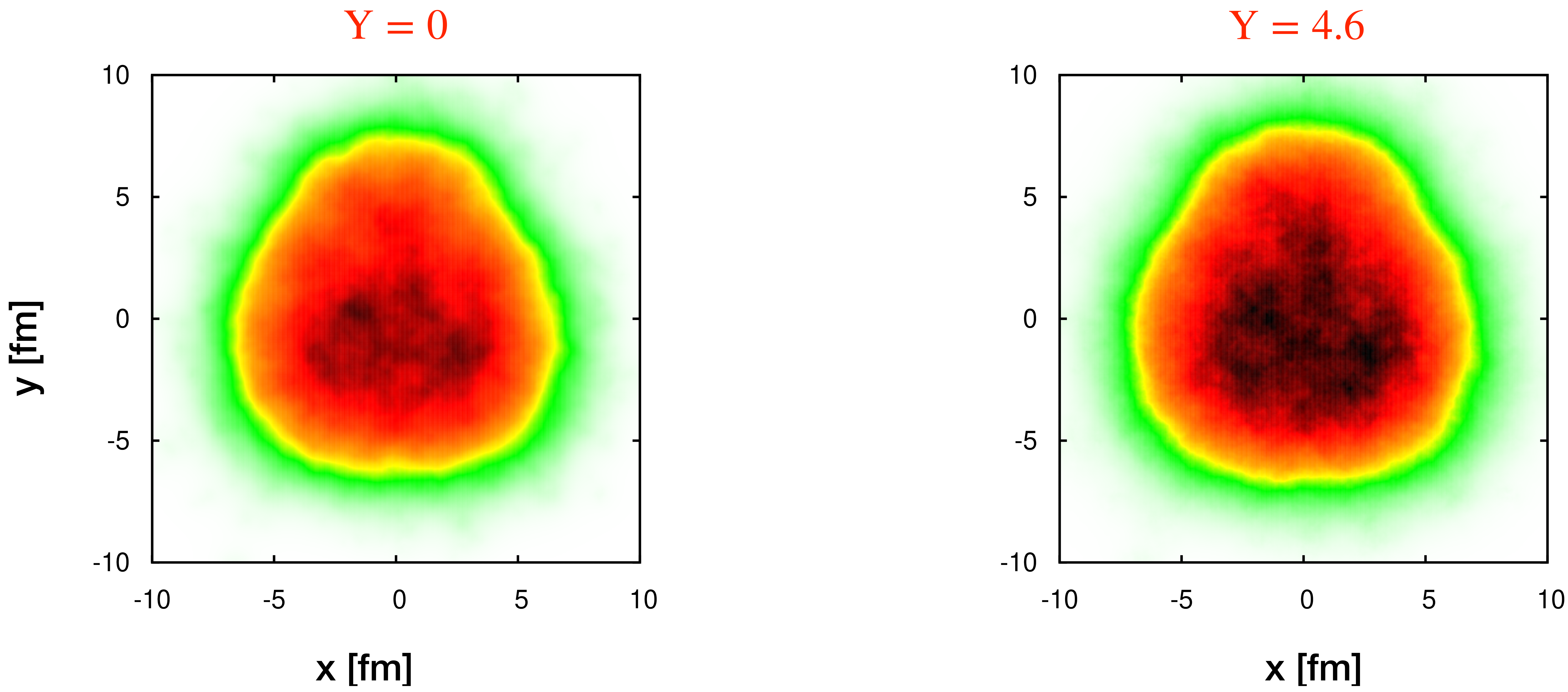

P. Singh

Effect of JIMWLK evolution on eccentricity

Using Wilson lines to calculate eccentricities for the fixed orientation

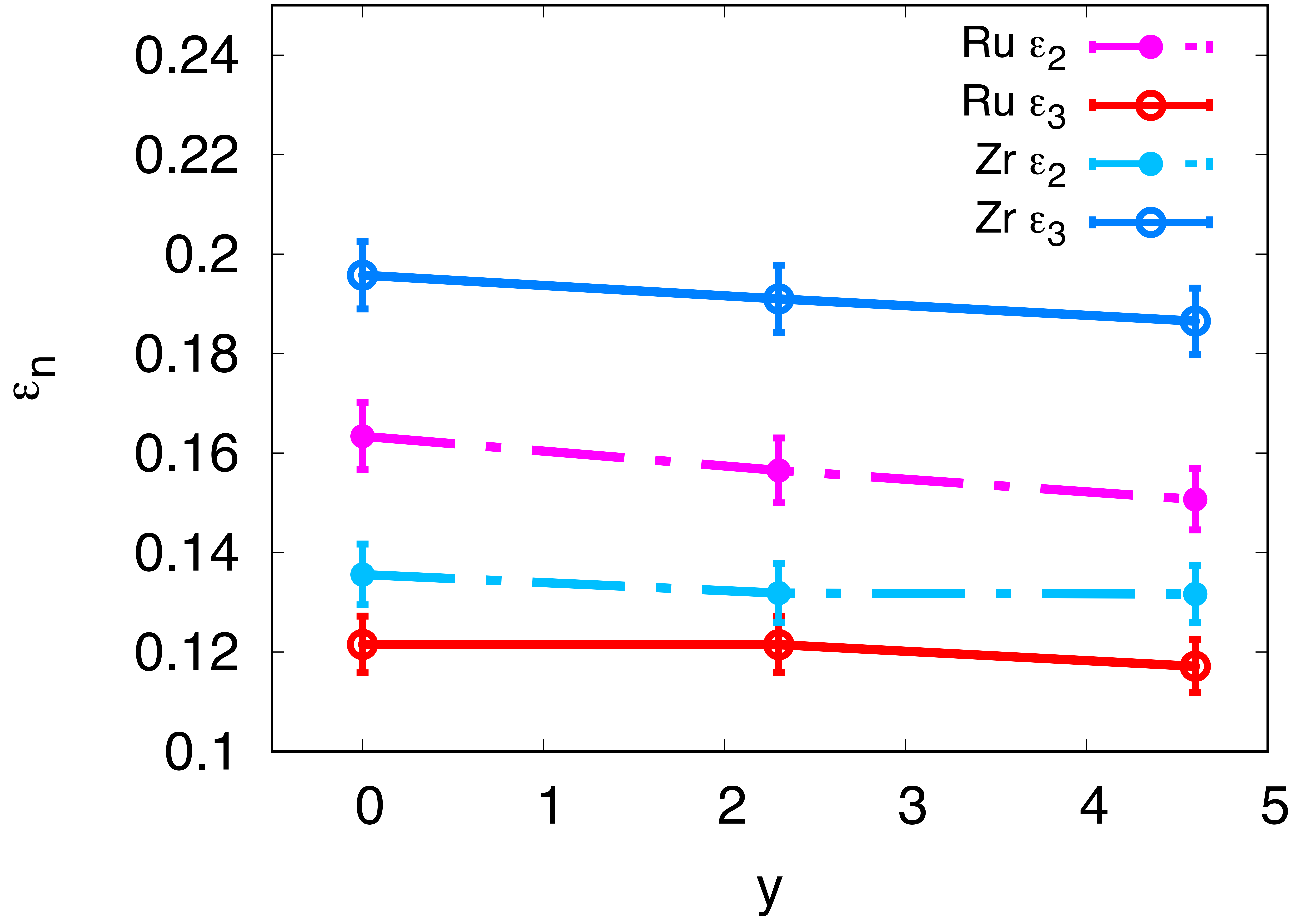

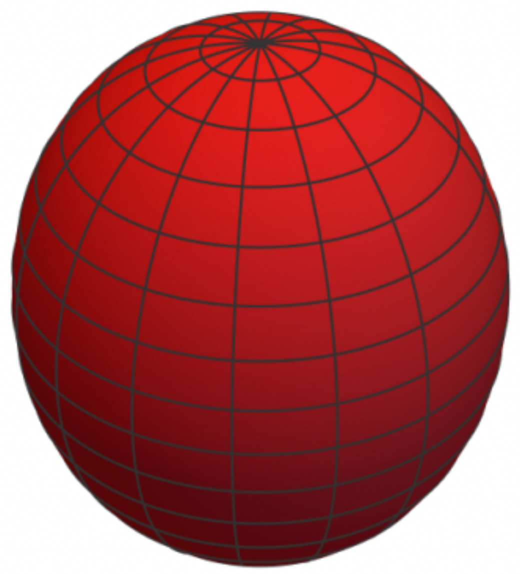

$^{96}_{44}$Ru

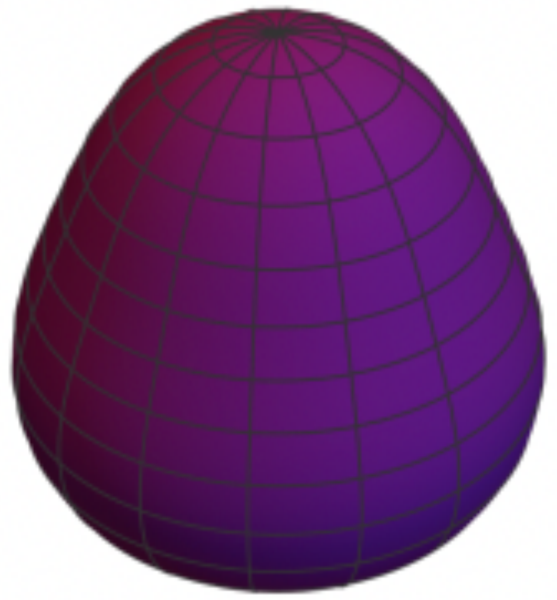

$^{96}_{40}$Zr

Summary

- Incoming nuclei described within color glass condensate: large x d.o.f. are color sources, small x classical gluon fields. We evolve the separation scale between the large and small-x dof.

- JIMWLK evolution leads to smoothening of geometric profile and growth in impact parameter space.

- Shape is modified by 10-20%

Future Prospect

- Isobar Runs: Ratio of observables

$$\frac{\mathcal{O}_{\mathrm{R}u}}{\mathcal{O}_{\mathrm{Z}r}} \approx 1 + c_0(R_{0,\mathrm{Ru}} - R_{0,\mathrm{Zr}}) + c_1(a_{0,\mathrm{Ru}} - a_{0,\mathrm{Zr}}) + c_2(\beta^2_{2,\mathrm{Ru}} - \beta^2_{2,\mathrm{Zr}}) + c_3(\beta^2_{3,\mathrm{Ru}} - \beta^2_{3,\mathrm{Zr}})$$

Jia & Zhang, arXiv:2111.15559
STAR collaboration, PRC 105 (2022) 1, 014901
Giacalone, Jia, Somà, PRC 104 (2021) 4, L041903

- Study of shape-size correlations using O-O collisions as a baseline

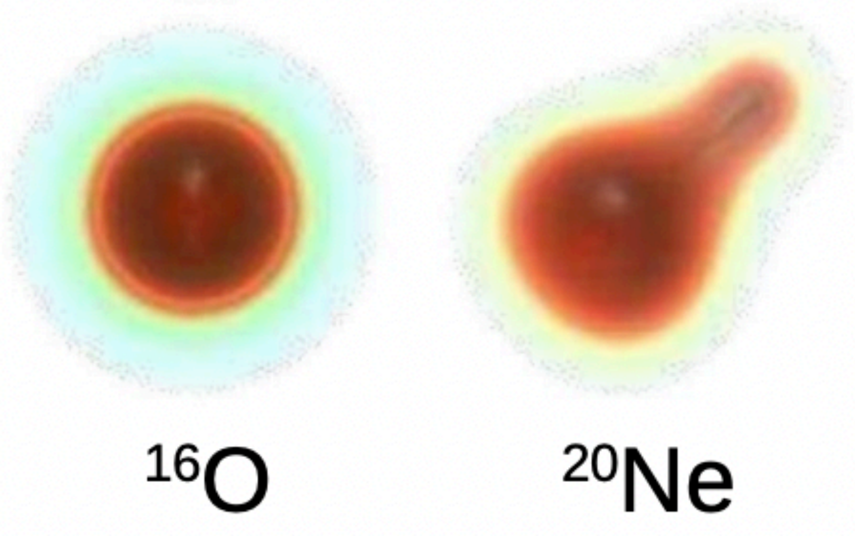

Thank you

BACKUP

Quantum evolution

- Quantum aspect refers to the evolution of the weight function with decreasing λ^+
- The field A^μ at momenta $k^+ \leq \lambda'^+$ is the sum $A^\mu = \mathscr{A}^\mu[\rho] + \delta A^\mu$ between the classical field $\mathscr{A}^\mu$ and the quantum fluctuations
- The averaging procedure involves two types of functional integrals
    - A classical integral over the color charge density ρ, which represents the fast partons with $k^+ \gg \lambda^+$
    - A quantum path integral over the gluon fluctuations δA^μ

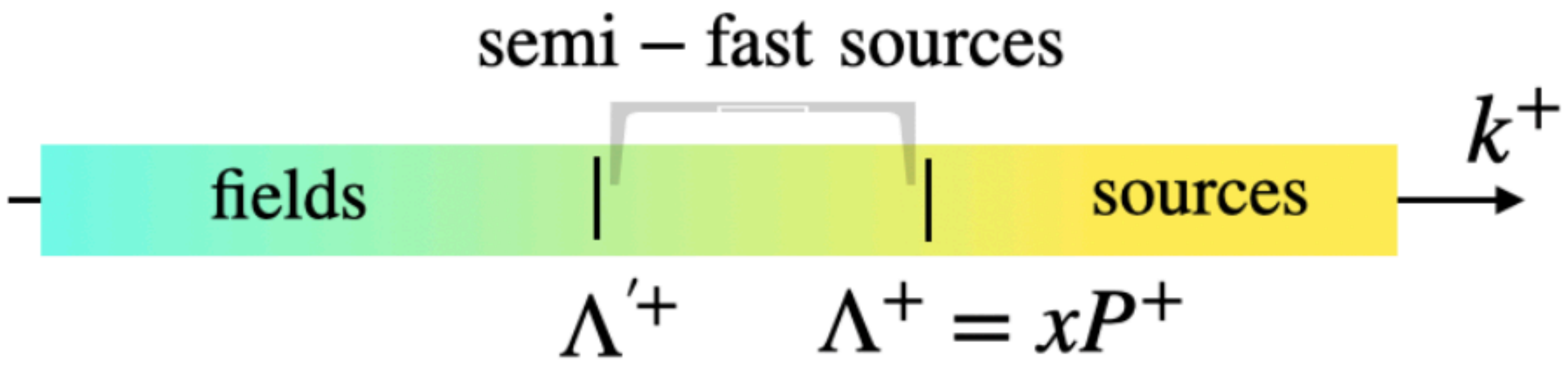

Gauge fields before the collision

L McLerran and R Venugopalan Phys. Rev. D 49, 3352

- Solution of Yang-Mills equation in covariant or $A^- = 0$ gauge is

$$A^+_{\rm cov}(x^-, x_\perp) = \frac{g\rho_1(x^-, x_\perp)}{\nabla^2_\perp + m^2}$$

- Solution in light-cone gauge is given as

$$A^+_{1,2}(x_\perp) = A^-_{1,2}(x_\perp) = 0$$

$$A^i_{1,2}(x_\perp) = \frac{i}{g} V_{1,2}(x_\perp)\partial^i V^\dagger_{1,2}(x_\perp)$$

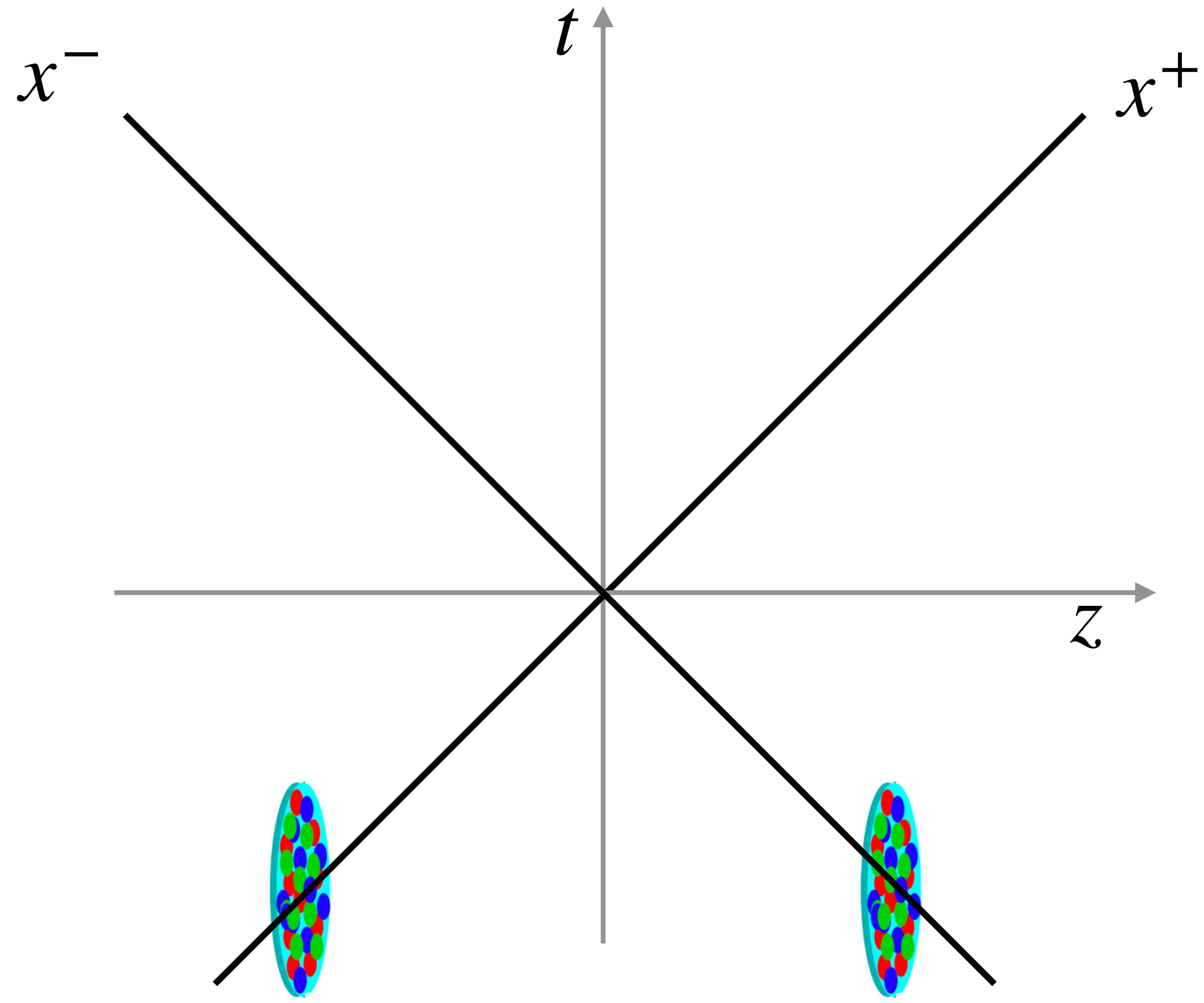

Nucleus 1

$J^+ = \rho_1(x^-, x_\perp)$

Nucleus 2

$J^- = \rho_2(x^+, x_\perp)$

Gauge fields after the collision

B Schenke, P Tribedy, and R Venugopalan Phys. Rev. C 86, 034908
A Krasnitz, R Venugopalan Nucl.Phys.B 557 (1999) 237

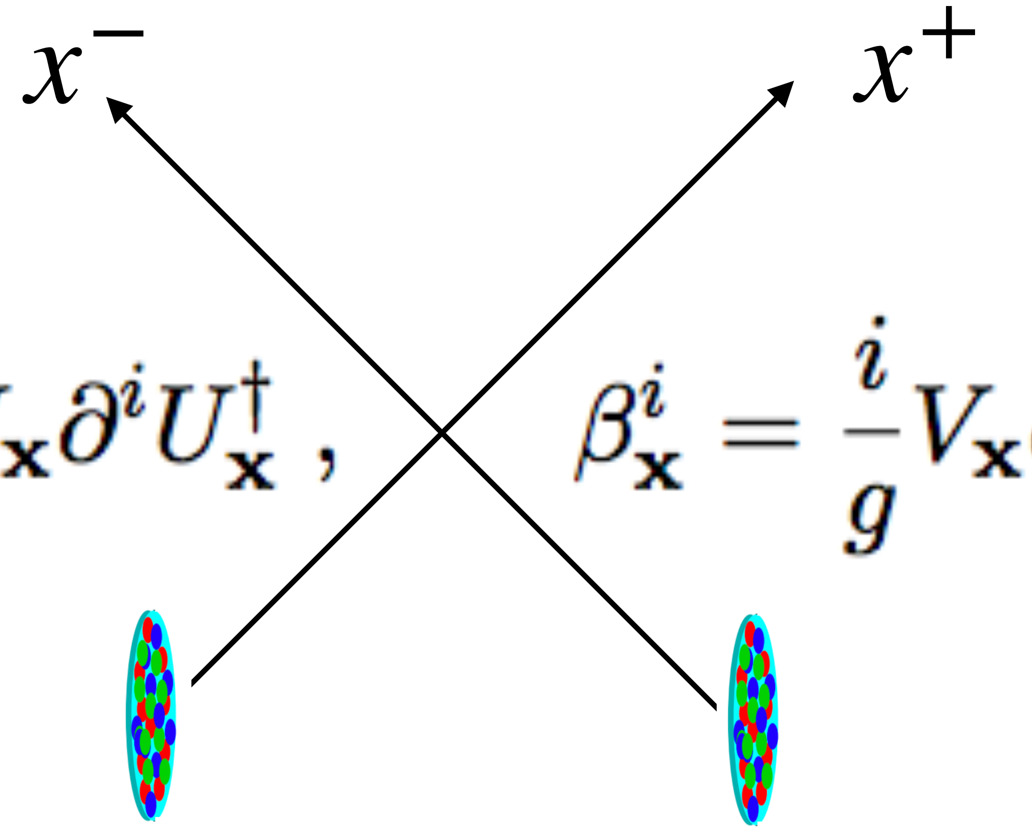

$$\alpha^i_{\mathbf{x}} = \frac{i}{g} U_{\mathbf{x}} \partial^i U^\dagger_{\mathbf{x}} \,, \qquad \beta^i_{\mathbf{x}} = \frac{i}{g} V_{\mathbf{x}} \partial^i V^\dagger_{\mathbf{x}} \,.$$

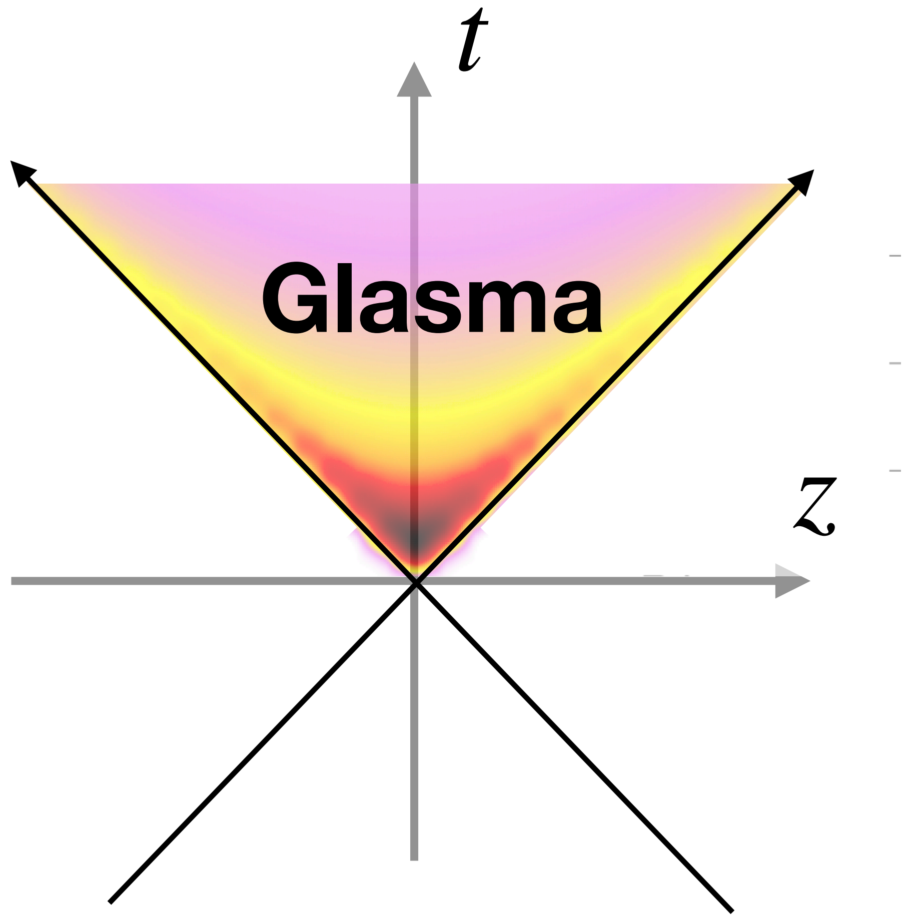

- α^i_x and $\beta^{\mathrm{i}}_{\mathrm{x}}$ are solution of YM in the light-cone gauge.
- Solution: $A^i_{x_\perp}(\tau = 0^+) = A^i_p(+y_{obs}) + A^i_{Pb}(-y_{obs});\quad A^\eta_{x_\perp}(\tau = 0^+) = \frac{i}{g}\left[A^i_p(+y_{obs}), A^i_{Pb}(-y_{obs})\right]$

Before the collision

Purely **transverse** chromo -electric and -magentic fields.

Immediately after collision

$$E^\eta_x = -ig\delta^{ij}[\alpha^i_x, \beta^j_x]$$

$$B^\eta_x = -ig\epsilon^{ij}[\alpha^i_x, \beta^j_x]$$

Subsequent evolution studied numerically using **2+1D source free classical Yang-Mills** simulations.

Color Glass Condensate: Sources and fields

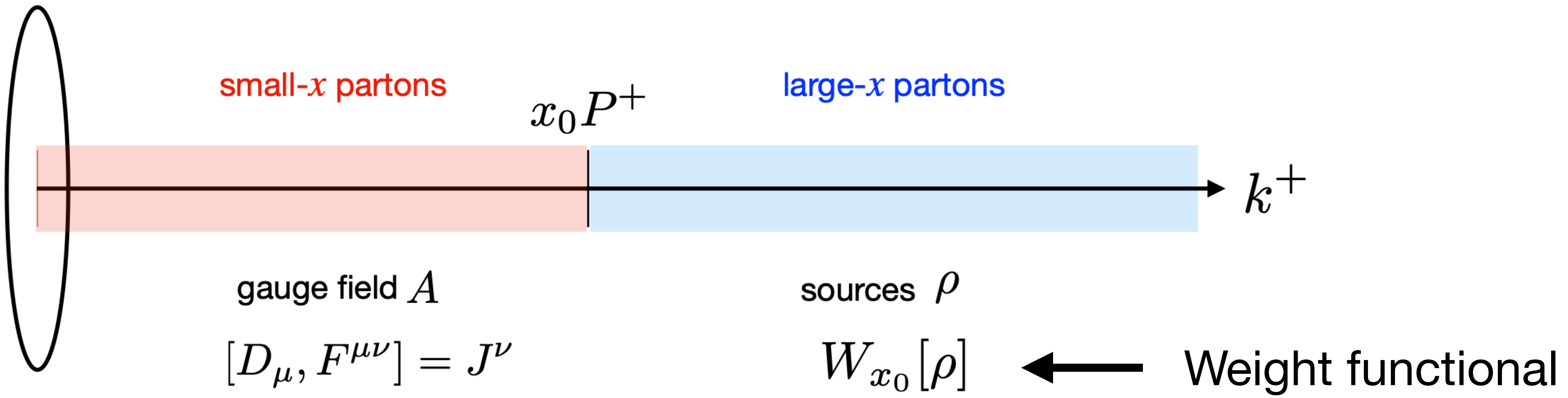

Two steps to compute expectation value of an observable $\mathcal{O}$:

1) Compute expectation value $\mathcal{O}[\rho] = \langle \mathcal{O} \rangle_\rho$ for sources drawn from a given $W_{x_o}[\rho]$

2) Average over all possible configurations given the appropriate gauge invariant weight functional $W_{x_o}[\rho]$

$$\langle \mathcal{O} \rangle_{x_0} = \int [\mathcal{D}\rho] W_{x_0}[\rho] \mathcal{O}[\rho] \,.$$

Ne-20 Random Orientated

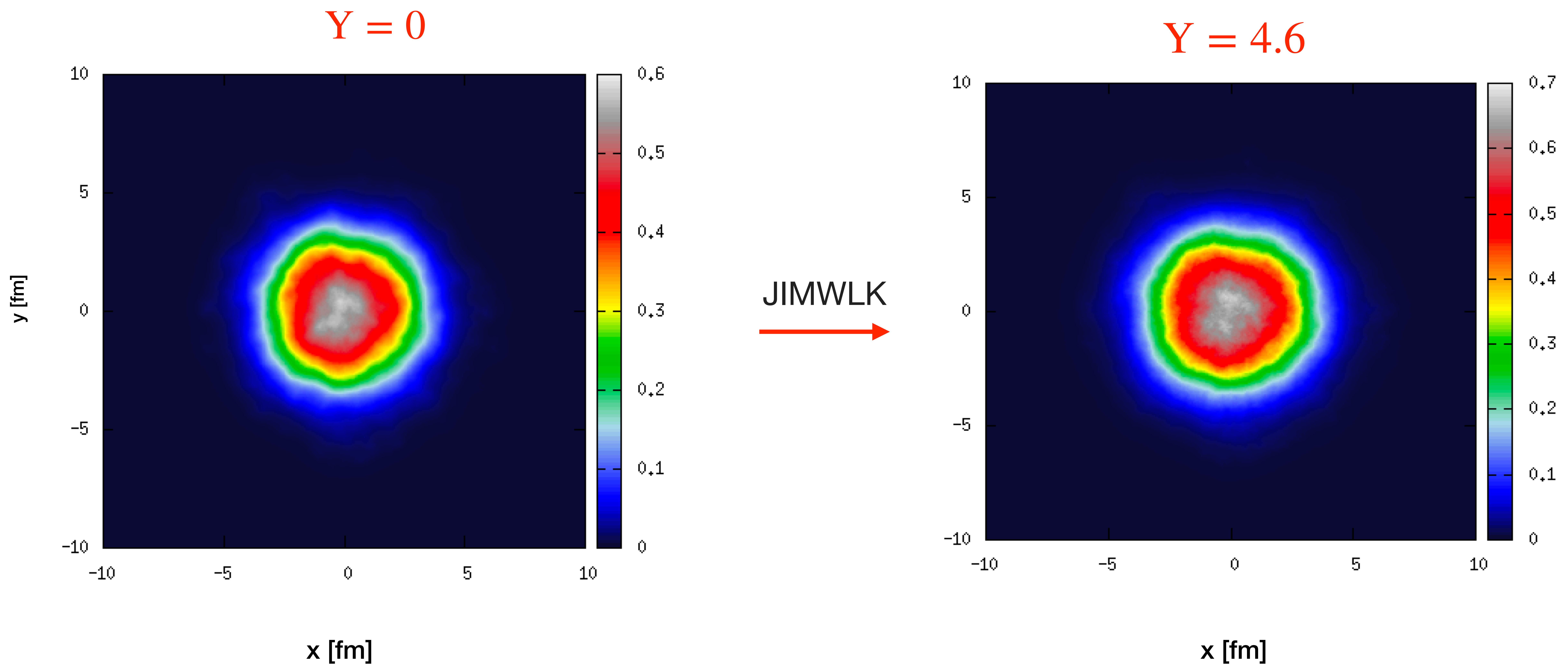

IPSAT

Kowalski, Teaney, Phys.Rev. D68 (2003) 114005

- The total cross section for a small dipole passing through a dilute gluon cloud is proportional to the dipole area, the strong coupling constant, and the number of gluons in the cloud: L. Frankfurt, A. Radyushkin, and M. Strikman, Phys. Rev. D55, 98 (1997)

$$\sigma_{q\bar{q}} = \frac{\pi^2}{N_c} r^2 \alpha_s(\mu^2) xg(x, \mu^2)$$

  where $xg(x, \mu^2)$ is the gluon density at some scale μ^2

- From that we get the Glauber-Mueller dipole cross section in a dense gluon system

$$\frac{d\sigma_{q\bar{q}}}{d^2 b} = 2(1 - \mathrm{Re} S(b)) = 2\left[1 - \exp\left(-\frac{\pi^2}{2N_c} r^2 \alpha_s(\mu^2) xg(x, \mu^2) T(b)\right)\right]$$

- $T(\mathbf{b})$ and $xg(x, \mu^2)$ are determined from fits to HERA DIS data (b, x, and initial scale μ_0^2 dependence) and DGLAP evolution in μ^2

GEOMETRY

- The thickness function $T(b)$ is modeled
- For a nucleon use a Gaussian or a collection of smaller Gaussians (substructure)

$$T(b) = \frac{1}{2\pi B_G} \exp\left(\frac{-b^2}{2B_G}\right)$$

- Usually B_G is assumed to be energy independent and fit yields $\sim 4\mathrm{GeV}^{-2}$
- It is related to the average squared gluonic radius $\langle b^2 \rangle = 2B_G$
- b is smaller than the charge radius: b=0.56 fm (c.f. R_p = 0.8751(61) fm)
- For a nucleus, do as in MC Glauber and sample nucleon positions from a nuclear density distribution (e.g. a Woods-Saxon distribution)
- Sum all nucleon $T(\vec{b})$ to get the total nuclear $T(\vec{b})$

GEOMETRY

from Schenke, Shen, Tribedy, Phys.Rev.C 102 (2020) 4, 044905

$$\rho(r,\theta) = \frac{\rho_0}{1+\exp[(r-R'(\theta))/a]}\,, \qquad (9)$$

with $R'(\theta) = R[1+\beta_2 Y_2^0(\theta)+\beta_4 Y_4^0(\theta)]$, and ρ_0 the nuclear density at the center of the nucleus. R is the radius parameter, a the skin depth.

Nucleus	R [fm]	a [fm]	β_2	β_4
^{238}U	6.81	0.55	0.28	0.093
^{208}Pb	6.62	0.546	0	0
^{197}Au	6.37	0.535	-0.13	-0.03
^{129}Xe	5.42	0.57	0.162	-0.003
^{96}Ru	5.085	0.46	0.158	0
^{96}Zr	5.02	0.46	0	0

Smaller nuclei, such as ^{16}O, and ^{3}He are described using a variational Monte-Carlo method (VMC) using the Argonne v18 (AV18) two-nucleon potential +UIX interactions [63]. In practice we use the ^{3}He and ^{16}O configurations available in the PHOBOS Monte-Carlo Glauber distribution [64, 65].

For the results we will show involving the deuteron, we employ a simple Hulthen wave function of the form [66]

$$\phi(d_{\rm pn}) = \frac{\sqrt{a_H b_H (a_H+b_H)}}{b_H - a_H}\,\frac{e^{-a_H d_{\rm pn}} - e^{-b_H d_{\rm pn}}}{\sqrt{2\pi}d_{\rm pn}}\,, \qquad (10)$$

where $d_{\rm pn}$ is the separation between the proton and the neutron, and the parameters are experimentally determined to be $a_H = 0.228\,{\rm fm}^{-1}$ and $b_H = 1.18\,{\rm fm}^{-1}$.

Color Glass Condensate: Sources and Fields

https://arxiv.org/pdf/hep-ph/0406169.pdf

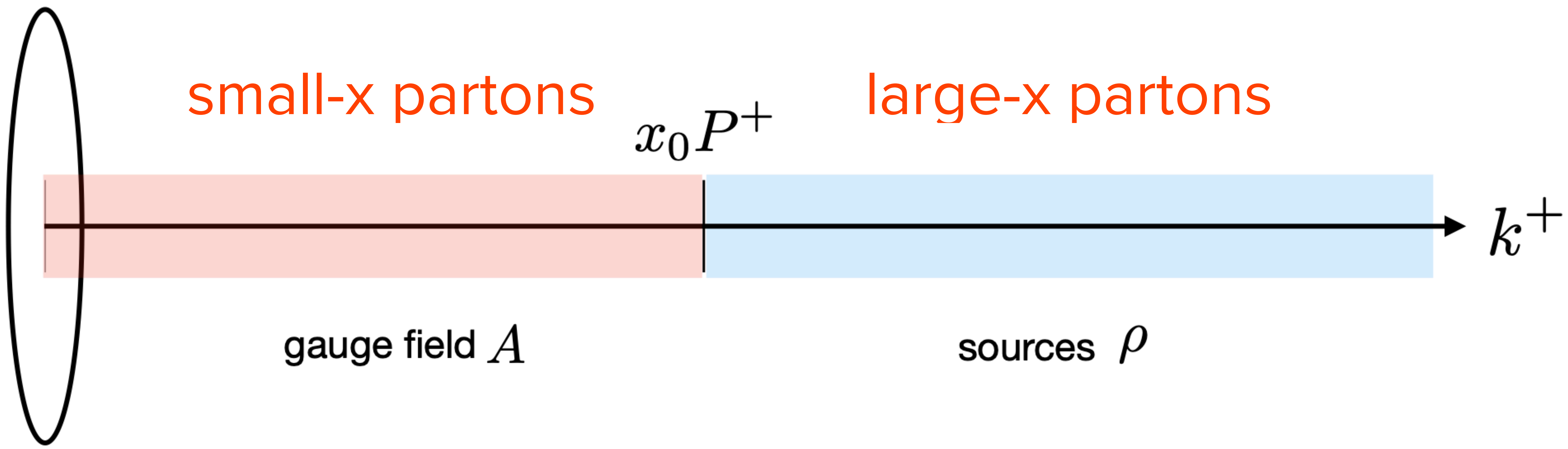

- Introduce the longitudinal momentum scale $\lambda^+ = x_0 P^+$ and differentiate between soft $(k^+ \leq \lambda^+)$ and hard $(k^+ > \lambda^+)$ degree of freedom.

- The strong separation in k^+ implies that the small-x and large-x dynamics decouple from each other and can be treated separately

IP-Sat : Color charge distribution inside Nuclei

IP-Sat (Impact Parameter dependent saturation) parametrization HERA DIS $\rightarrow$ proton-dipole scattering matrix $S^p_{\rm dip}(\mathbf{r}_\perp, x, \mathbf{b}_\perp) \sim \exp\left(-r^2 Q^2_{sp}/2\right)$

The nuclear scattering matrix is obtained as

$$S^A_{\rm dip}(\mathbf{r}_\perp, x, \mathbf{b}_\perp) = \prod_{i=0}^{A} S^p_{\rm dip}(\mathbf{r}_\perp, x, \mathbf{b}_\perp)$$

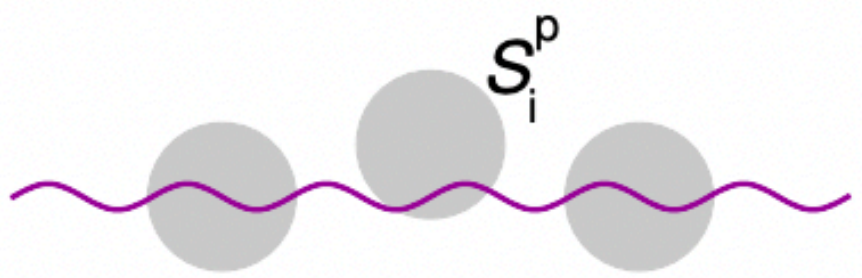

$i \rightarrow$ nucleons are distributed according to Fermi distribution.

$S^A_{\rm dip} \rightarrow$ distribution of nuclear saturation scale $Q_s(\mathbf{b}_\perp, x)$ solving :

$$S^A_{\rm dip}(\mathbf{r}_\perp = r_S, x, \mathbf{b}_\perp) = \exp(-1/2) \implies Q_s^2 = \frac{2}{r_S^2}$$

Iteratively solving $x = \frac{Q_s(\mathbf{b}_\perp, x)}{\sqrt{s}} \rightarrow Q_s(\mathbf{b}_\perp, \sqrt{s})$

Lumpy color charge density distribution $g^2\mu(\mathbf{x}_\perp) \sim Q_s(\mathbf{x}_\perp)$

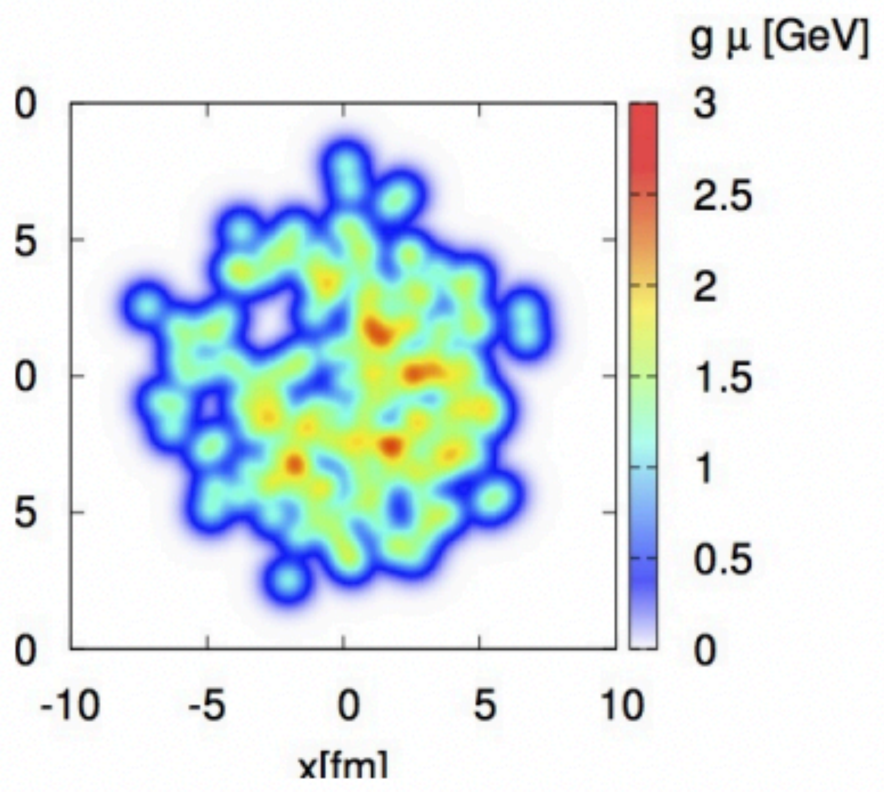

Kowalski, Lappi, Venugopalan 0705.3047

Effect of JIMWLK evolution on small systems

Result for Ne-20 eccentricities using Wilson lines

$$\Delta y = log\left(\frac{\sqrt{s}_H}{\sqrt{s}_L}\right)$$

$$\epsilon_n(y) = \frac{\int d^2\mathbf{r}_\perp(1 - \mathrm{ReTr\ V(y, \mathbf{r}_\perp)})\,|\,\mathbf{r}_\perp|^{\mathrm{n}}\,\mathrm{e}^{\mathrm{i}n\phi_{\mathrm{n}}}}{\int d^2\mathbf{r}_\perp(1 - \mathrm{ReTr\ V(y, \mathbf{r}_\perp)})\,|\,\mathbf{r}_\perp|^{\mathrm{n}}}$$

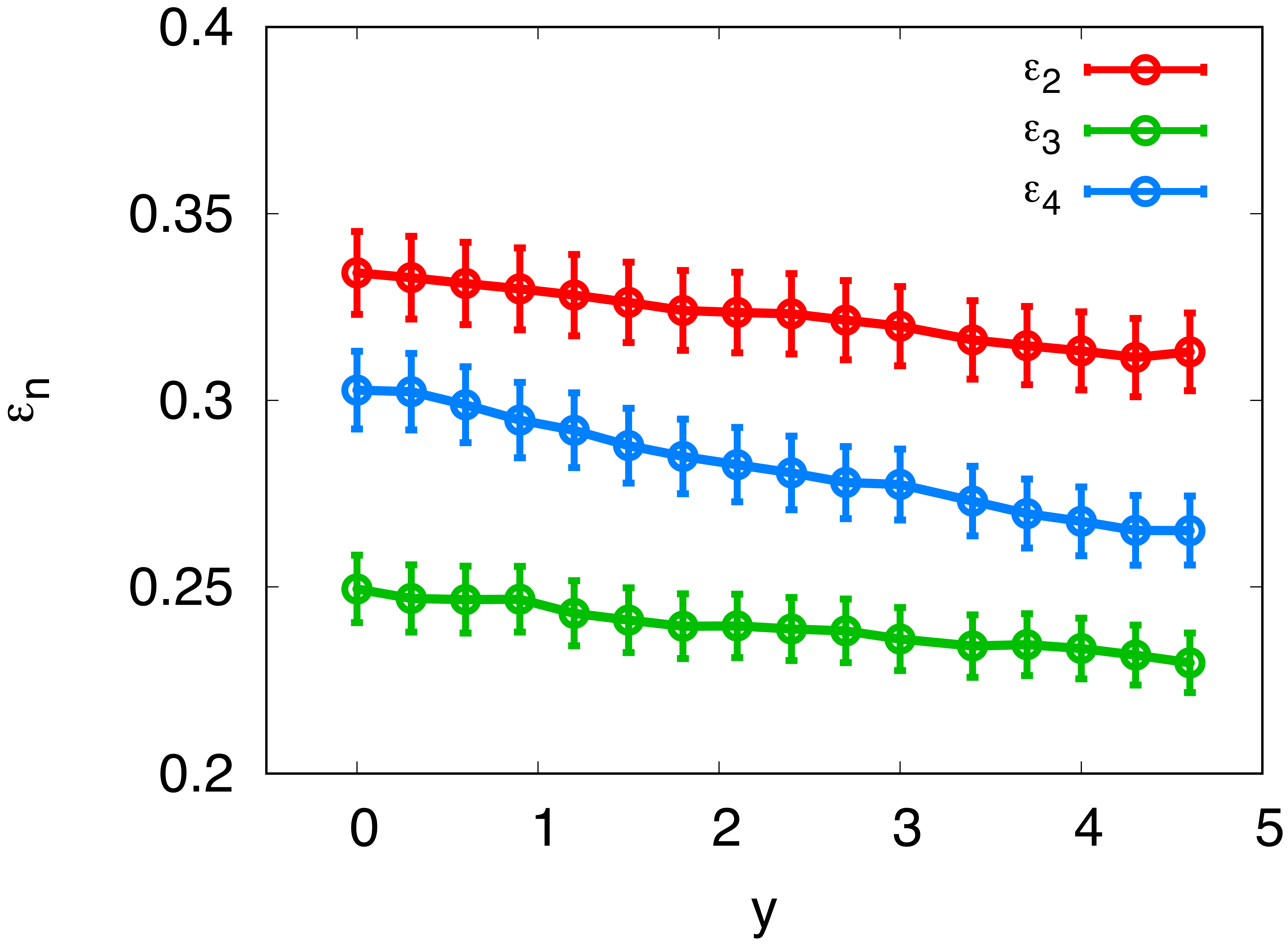

Generating color charge density

- The valence quarks are randomly distributed such that the total charge seen by the probe satisfies

$$\langle Q^a \rangle = 0 \qquad \langle Q^a Q^a \rangle \propto g^2 N$$

- If N is large, these color charges can be treated as **classical**

- Introducing color charge densities $\rho(x^-, x_\perp)$

$$Q^a = \int_{S_\perp} d^2x \rho^a(x) = \int_{S_\perp} d^2x \int dx^- \rho^a(x^-, x_\perp)$$

- Based on central limit theorem, the color charge density will have a simple Gaussian probability distribution. The one- and two-point function

$$\langle \rho^a(x_\perp) \rangle = 0$$

$$\langle \rho^a(x_\perp) \rho^b(y_\perp) \rangle = g^2 \mu^2 \delta^{ab} \delta^{(2)}(x_\perp - y_\perp)$$

where μ^2 is the average color charge squared of the valence quarks per unit transverse area